X-ray Observations of Lighthouse Pulsar Wind Nebula and its remarkable filament.

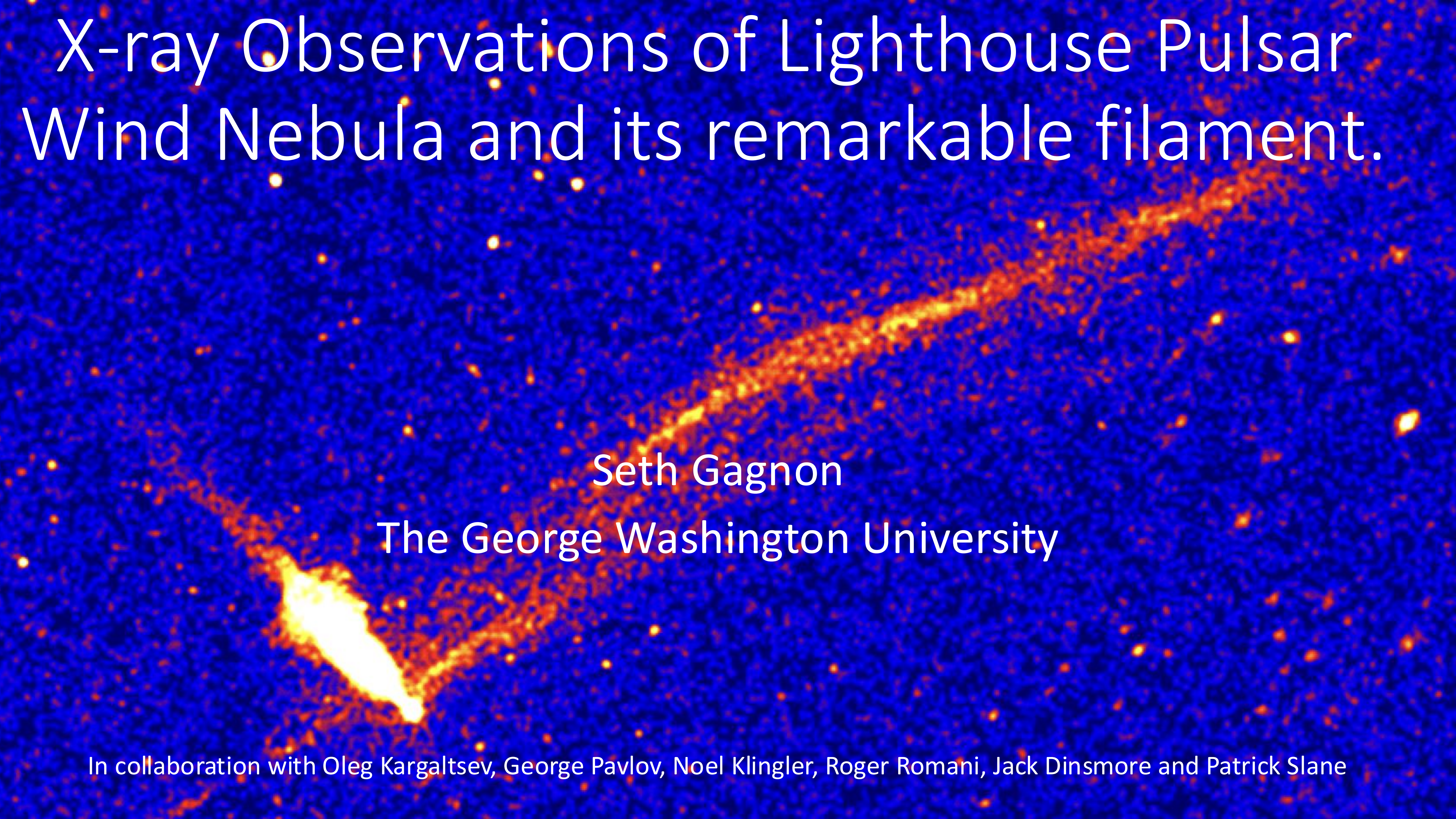

Seth Gagnon

The George Washington University

In collaboration with Oleg Kargaltsev, George Pavlov, Noel Klingler, Roger Romani, Jack Dinsmore and Patrick Slane

PWNe of supersonic pulsars

- PWN morphology is determined by Mach number
  - $\mathcal{M} = v_{PSR}/c_{s,ISM}$
- supernovae explosions are asymmetrical → typical pulsar kick velocities
  - $v_{PSR} \sim$ few × 100 km/s
- inside SNRs: PSRs are subsonic
  - wind is anisotropic → polar + equatorial outflows (jets + torus)
- outside SNRs: PSRs usually supersonic
  - $c_{s,ISM} \sim$ a few – a few × 10 km/s
  - ISM exerts ram pressure on wind → bow shock forms
    - wind confined behind PSR, structures deformed, extended tails

Axial symmetry (torus + jets) usually seen

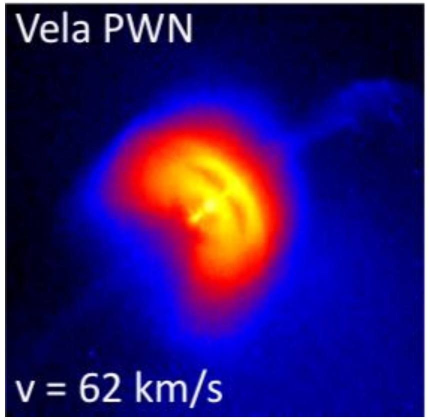

$\mathcal{M} < 1$: jets/tori visible

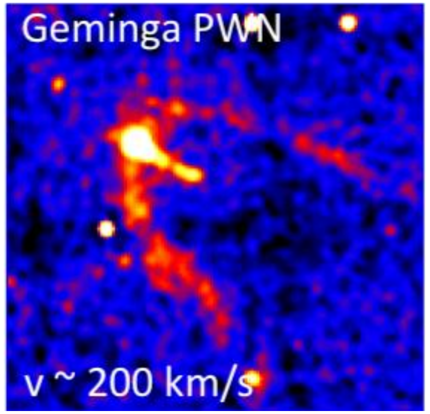

$\mathcal{M} \gtrsim 1$: jets/tori get bent back

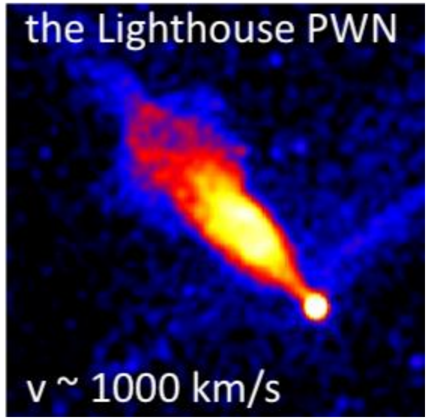

$\mathcal{M} \gg 1$: jets/tori get crushed + mixed

TS – termination shock
CD – contact discontinuity
FS – forward shock

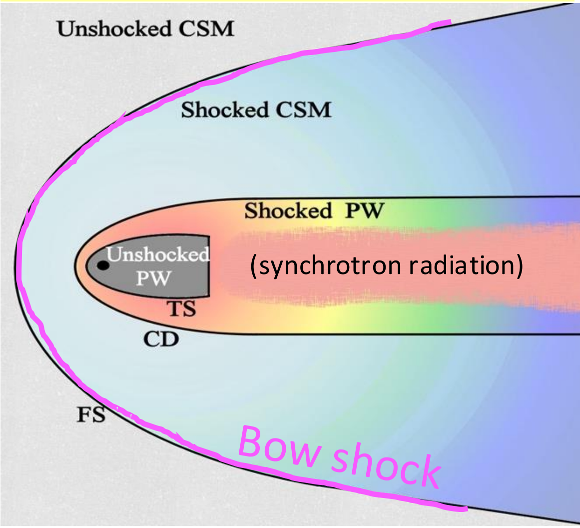

PWN Zoo (as seen by Chandra)

subsonic

$\mathcal{M} < 1$: jets/tori visible (usually)

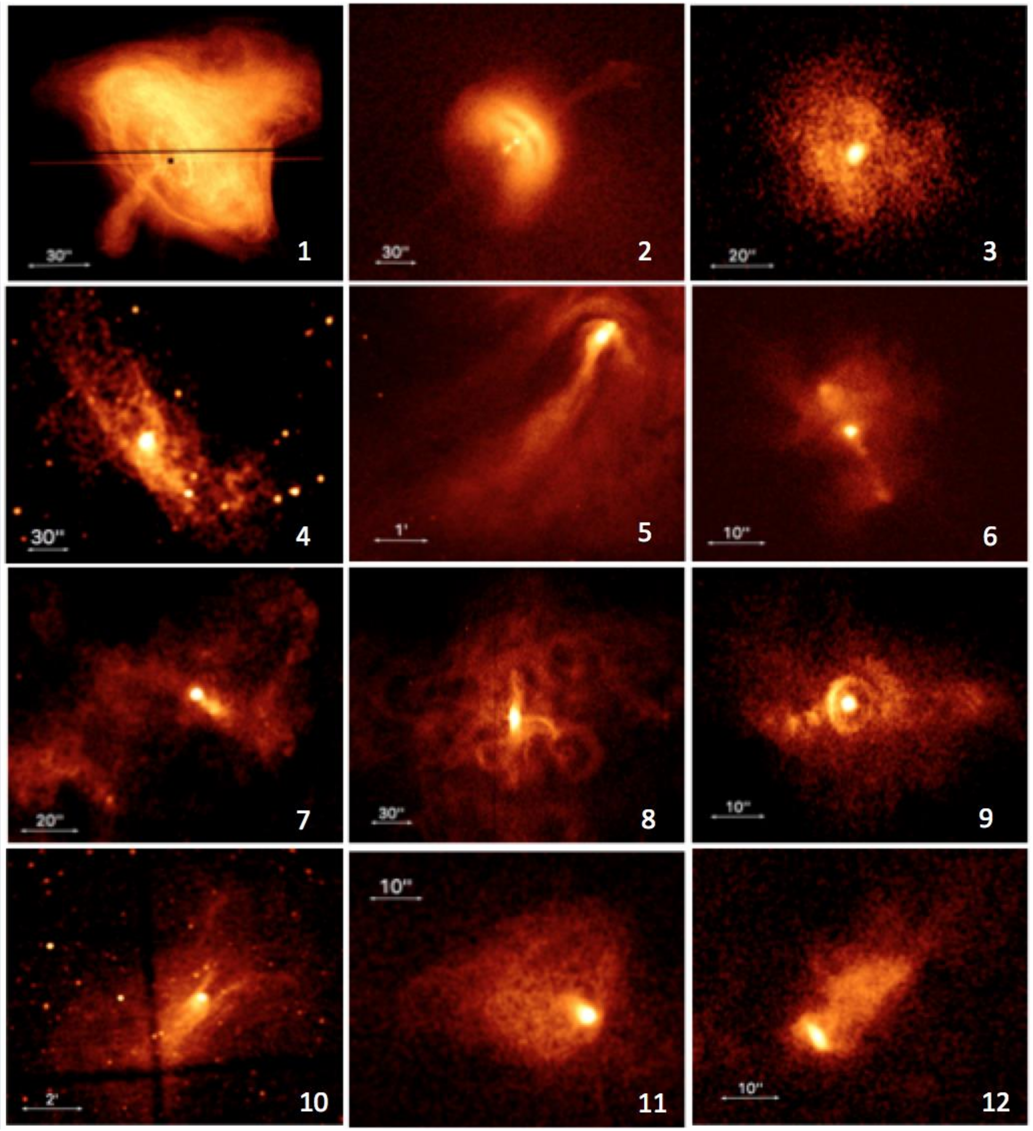

$\mathcal{M} \gtrsim 1$: jets/tori bent by ram pressure

$\mathcal{M} \gg 1$: wind is crushed + mixed together

supersonic

bow shock compact nebulae + extended tails

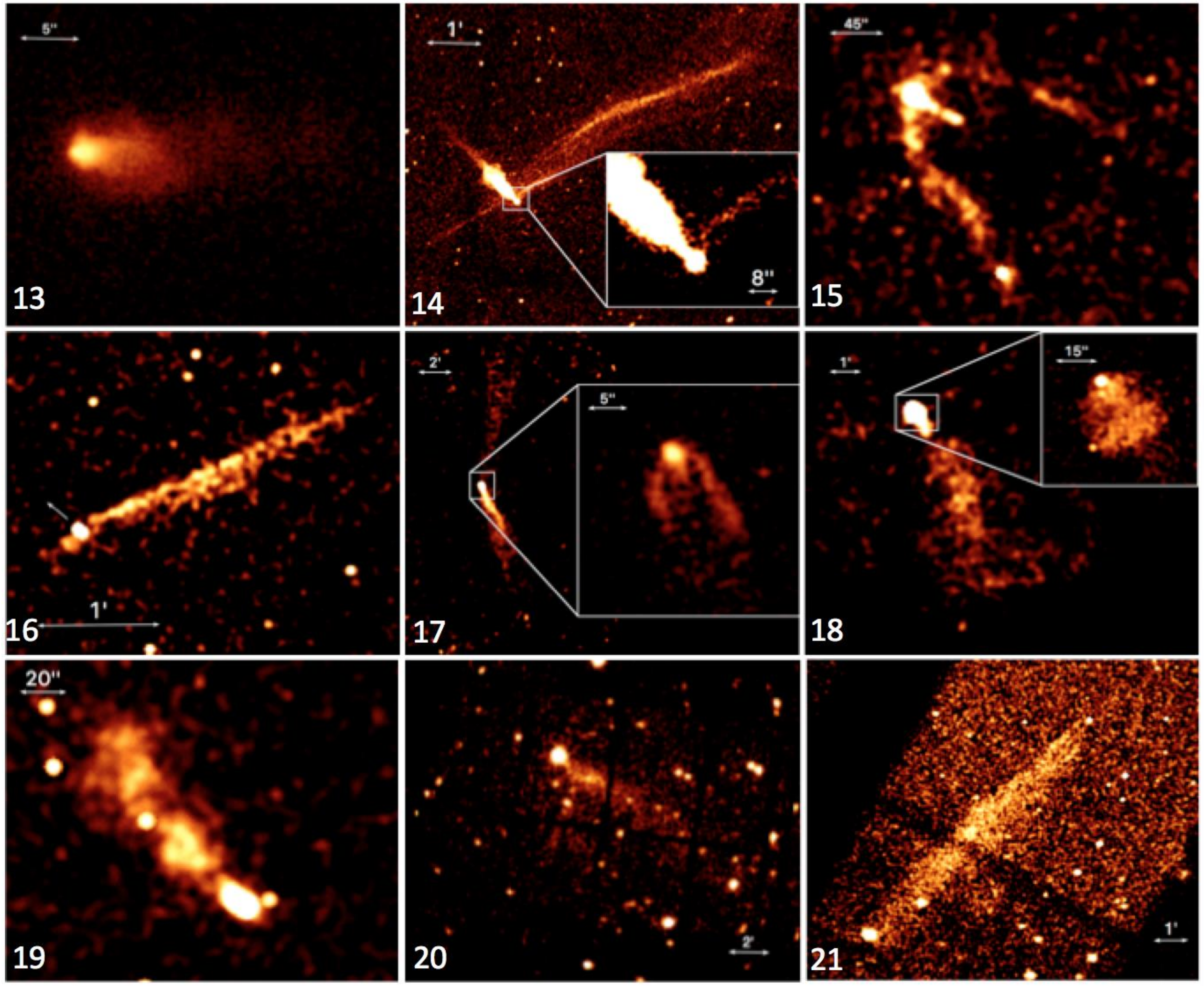

Highly Supersonic PWNe

$\dot{E} = 5.1 \times 10^{35}$ erg s
$\tau_c = 154$ kyrs
$B_s = 9.1 \times 10^{11}$ G

A shallow image only showed compact PWN with two tails (similar to Geminga)
Deeper image showed a longer tail behind the moving pulsar.
An even deeper image reveals the puzzling **misaligned** (with pulsar velocity) **outflow (a.k.a. pulsar x-ray filament).**

PSR J1509-5850

ACIS 370 ks

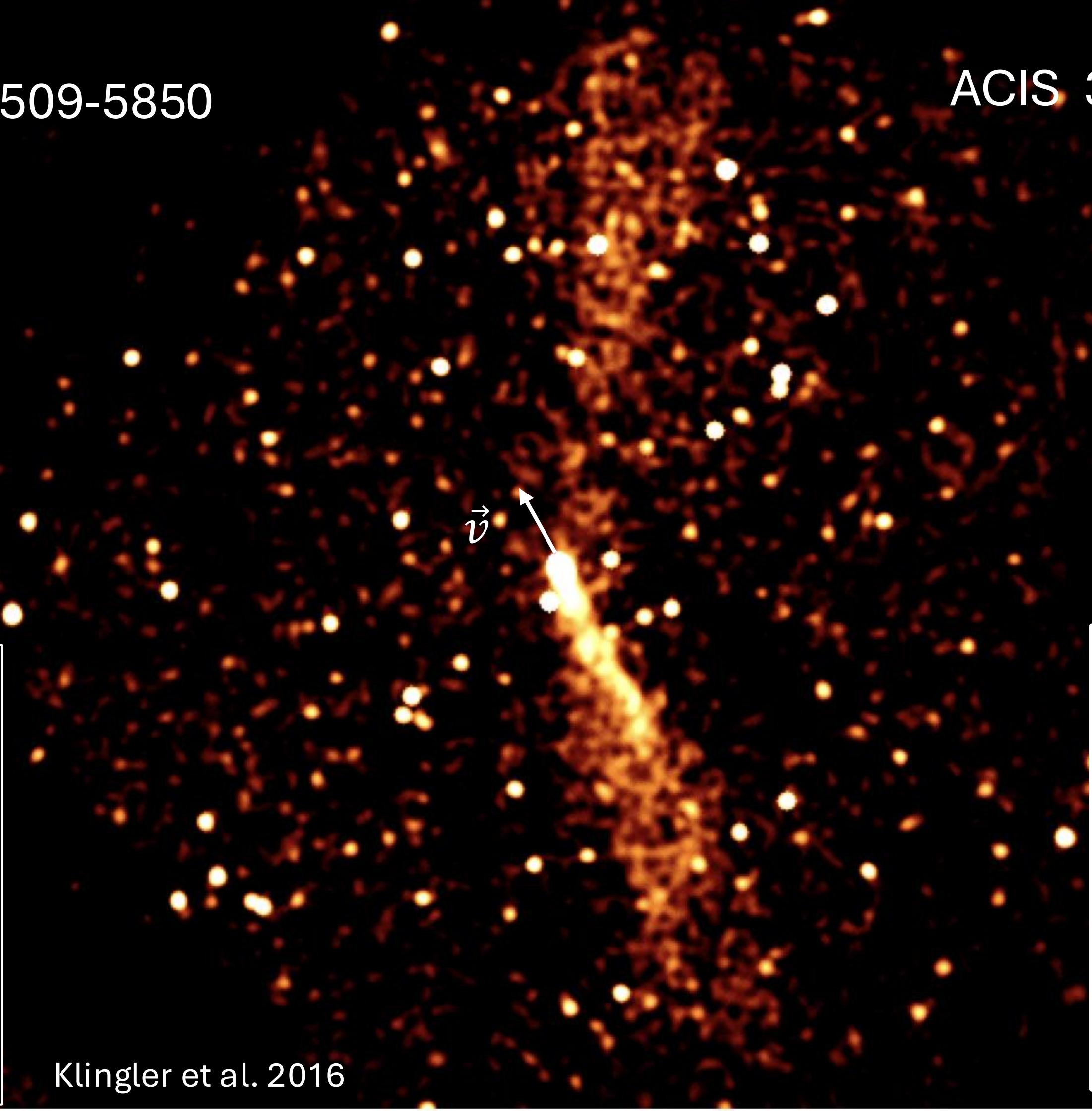

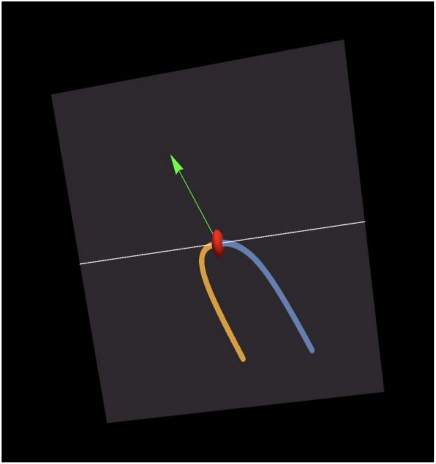

Klingler et al. 2016

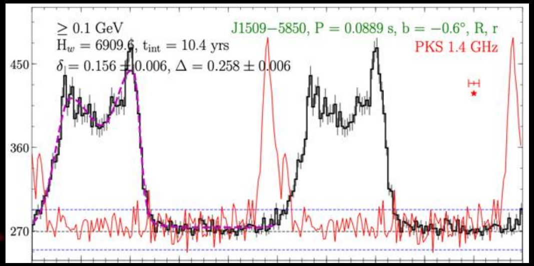

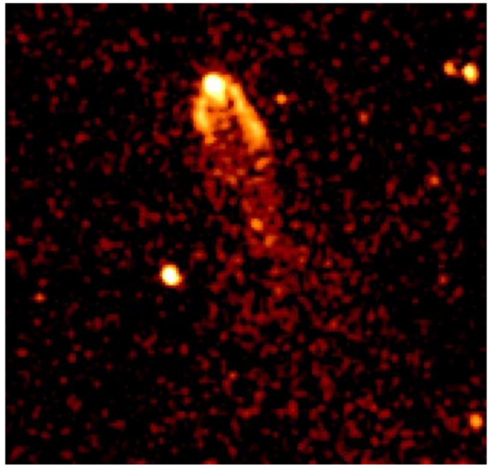

Radio images only show the tail and not the filament

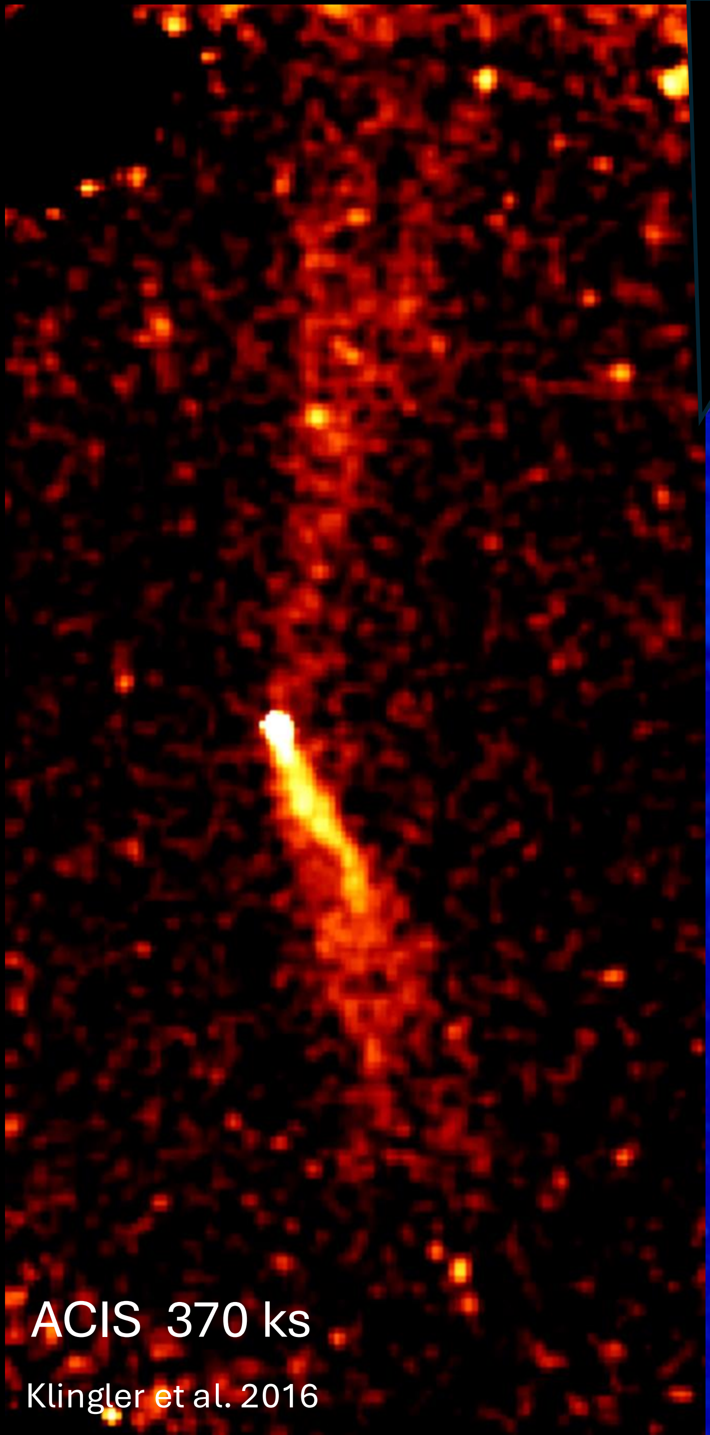
ACIS 370 ks

Klingler et al. 2016

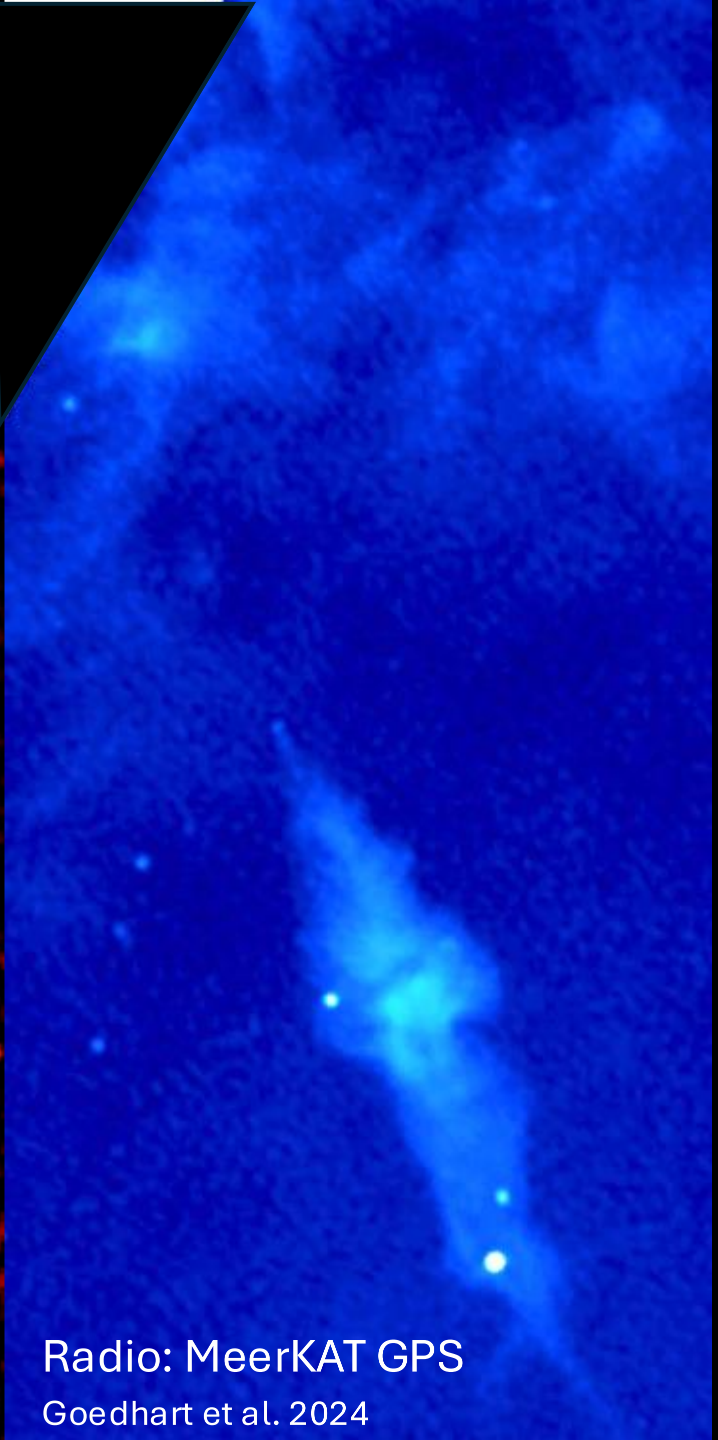
Radio: MeerKAT GPS

Goedhart et al. 2024

The Lighthouse nebula

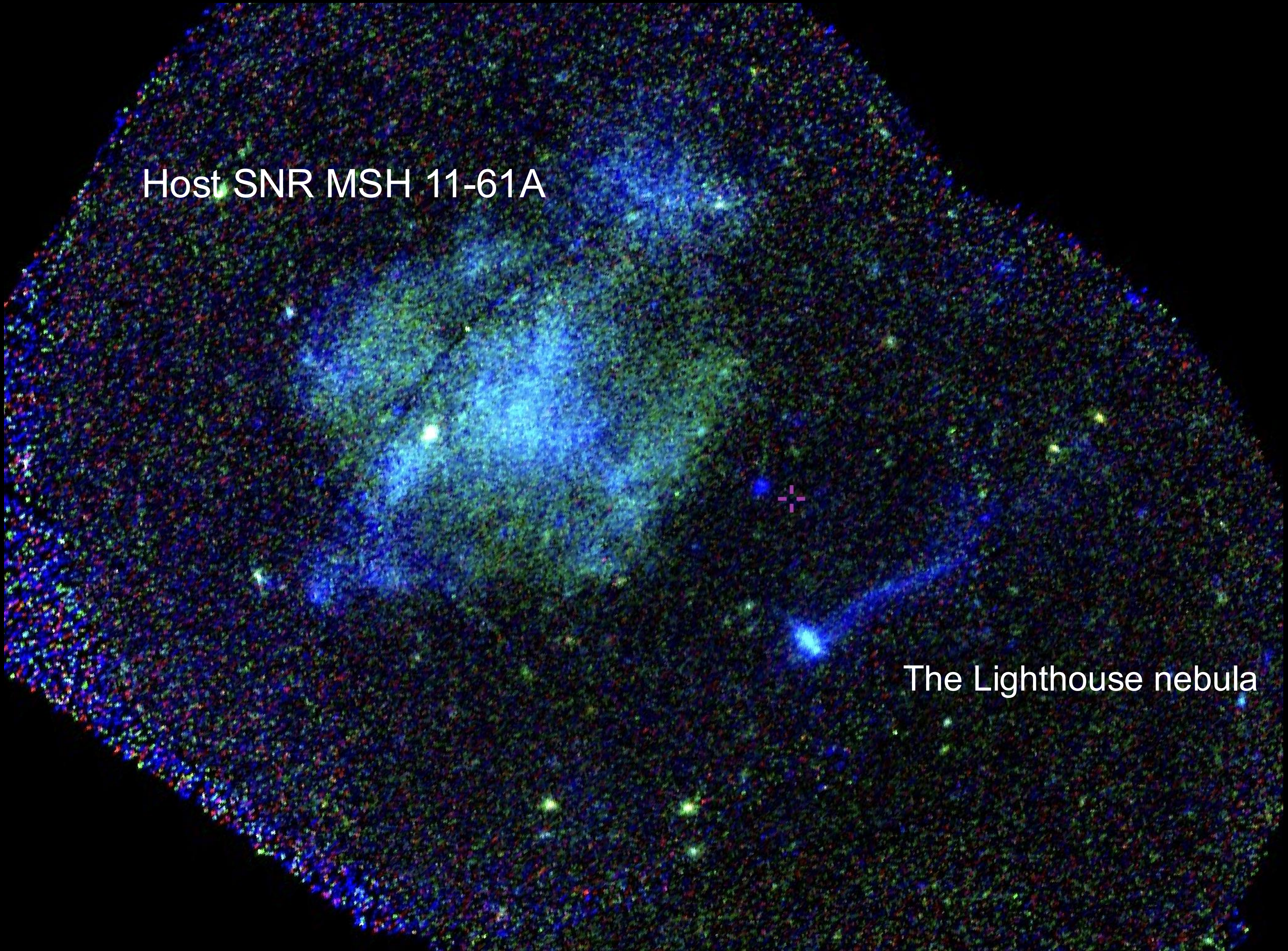

The Lighthouse nebula

A spectacular pulsar filament of a highly supersonic PWN

PSR J1101–6101

$\dot{E} = 1.4 \times 10^{36}$ erg s^{-1}
$\tau_c = 116$ kyrs
$B_s = 7.4 \times 10^{11}$ G
d=6.3 kpc

radio & γ-ray quiet

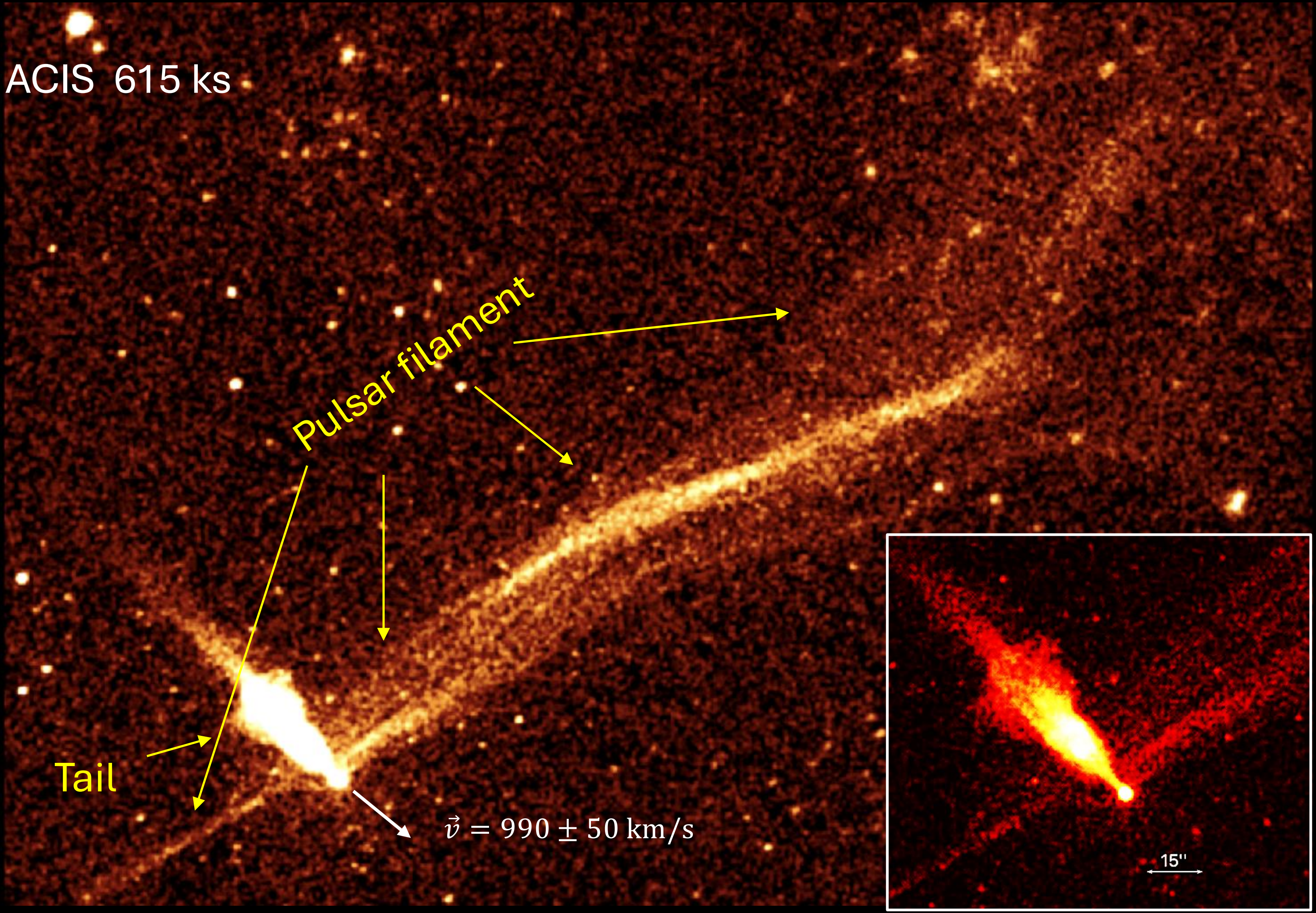

Tomsick et al. 2012, Pavan et al. 2016, Klingler et al. 2023, Dinsmore & Romani 2006

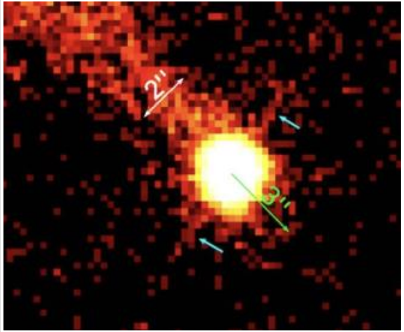

Magnetic draping

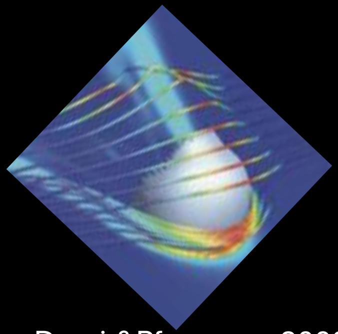

Dursi &Pfrommer 2008

IXPE observations show the magnetic field runs parallel to the filament

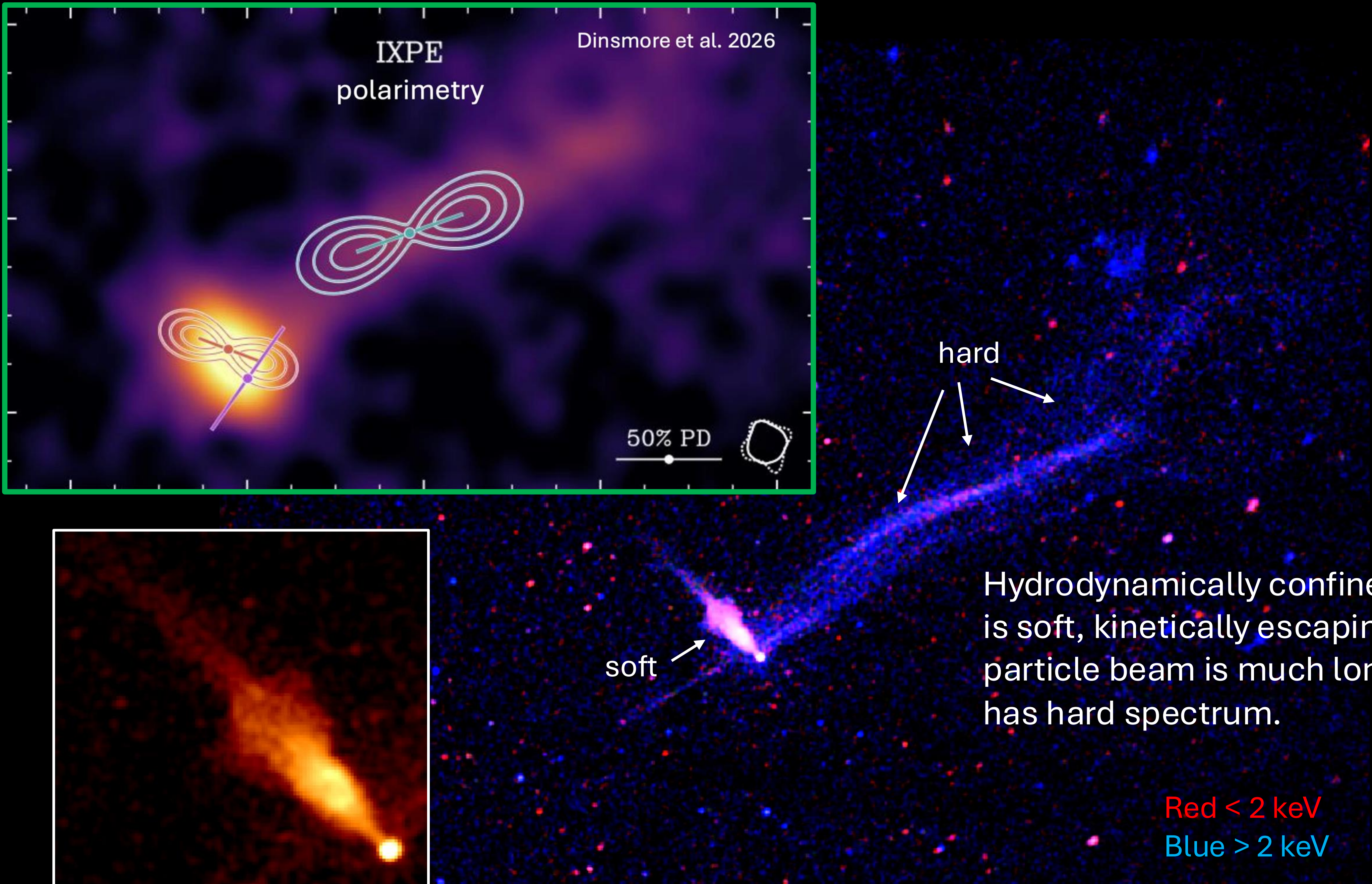

Dinsmore et al. 2026

Hydrodynamically confined tail is soft, kinetically escaping particle beam is much longer, has hard spectrum.

Red < 2 keV
Blue > 2 keV

The deep radio image only shows the tail but not the misaligned outflow

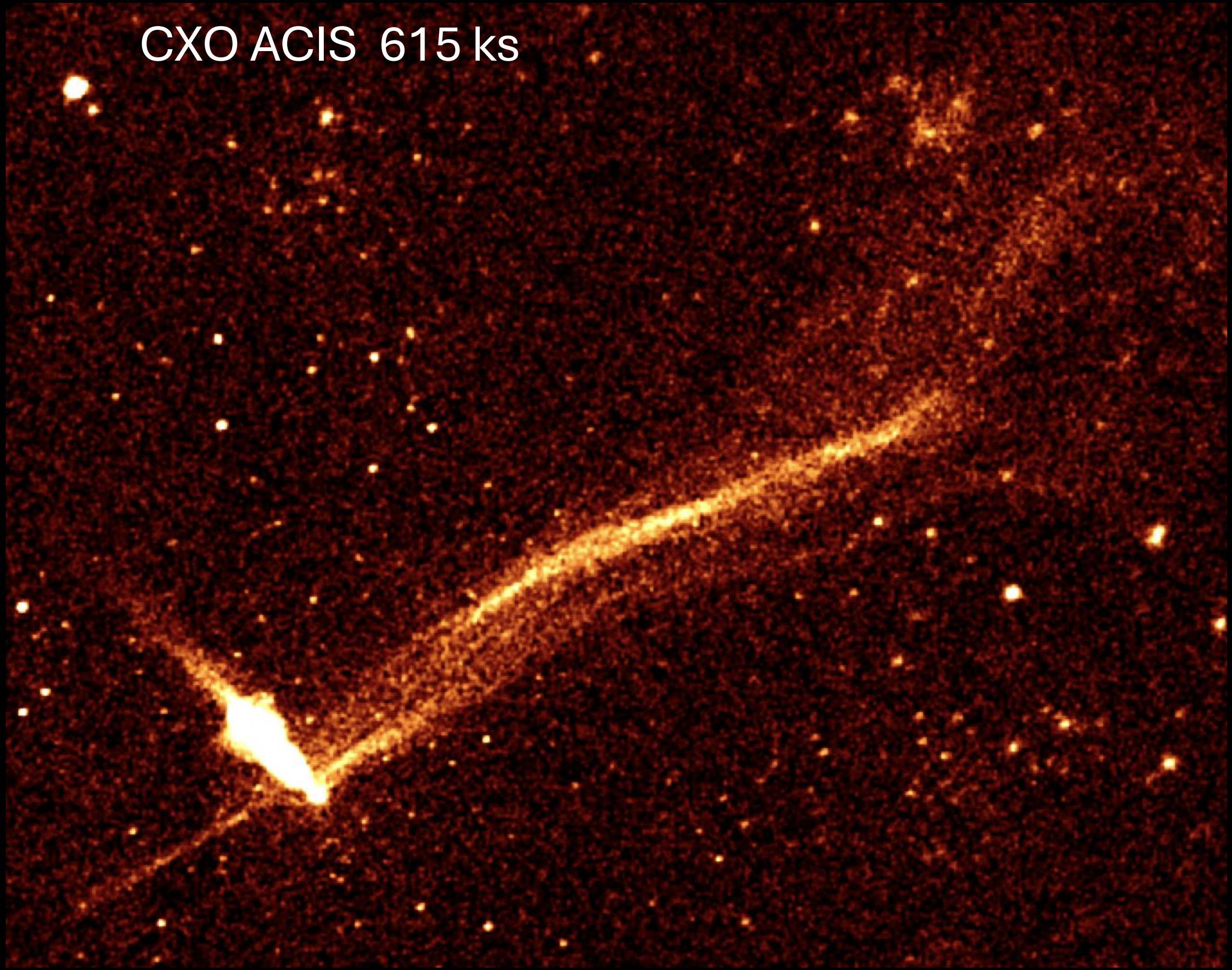

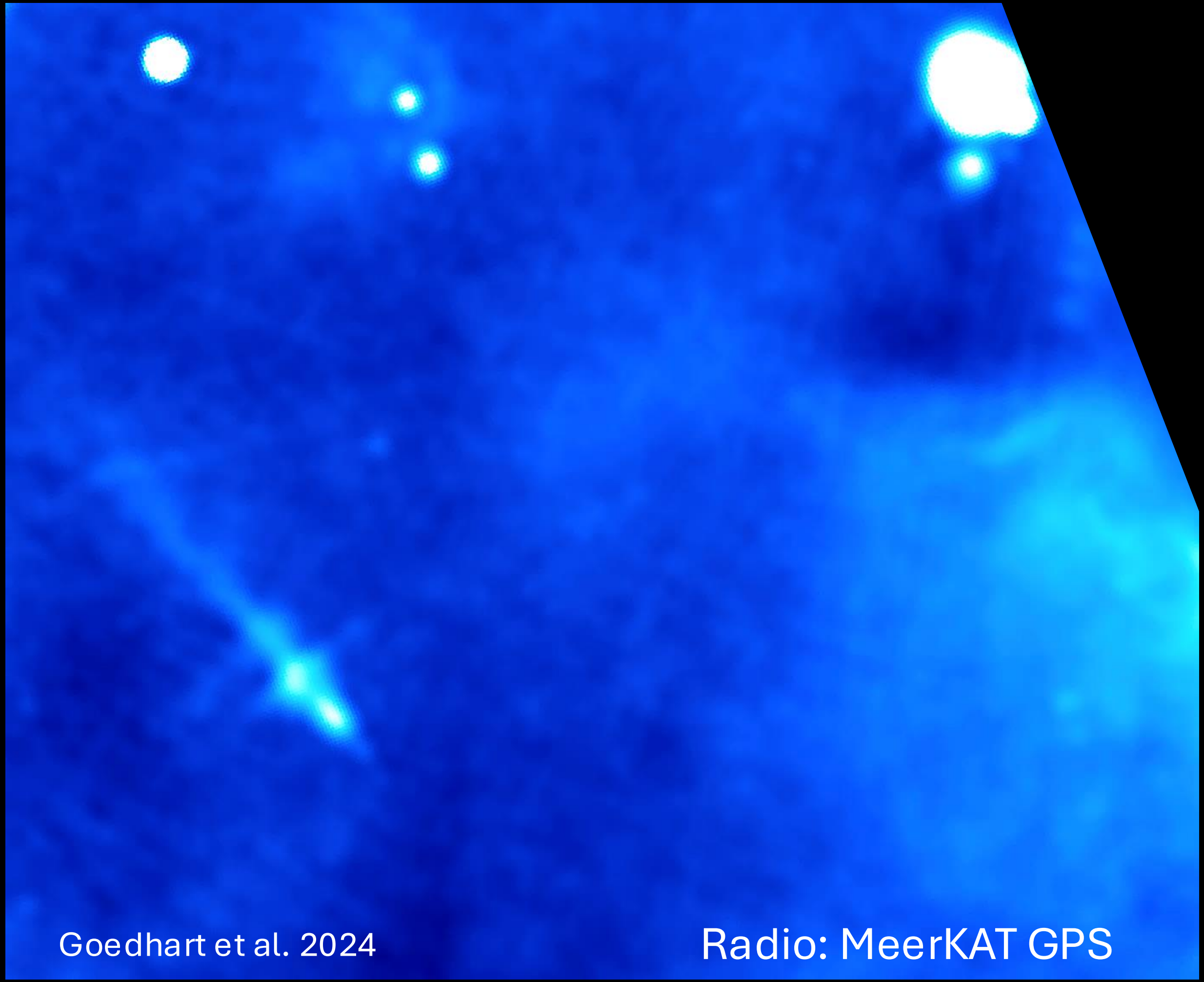
Goedhart et al. 2024

Misaligned Outflows: Theory

- possible explanation: if gyration radius (r_g) of energetic e^-/e^+ exceeds size of bow shock apex (r_{BS}), particles can escape into ISM (Bandiera 2008)
- e^-/e^+ accelerated via B_{psr} /B_{ISM} reconnection
- e^-/e^+ then travel along + illuminate ISM field lines; misalignment reflects direction of external B-field
- observations support theory:
  - not seen in radio because $r_g < r_{BS}$
  - one-sided due to reconnection
  - spectra are hard
    - $\Gamma_{lighthouse} = 1.6 \pm 0.2$
    - $\Gamma_{guitar} = 1.30 \pm 0.11$
    - $\Gamma_{J1509} = 1.81 \pm 0.10$
    - $\Gamma_{B0355} = 1.60 \pm 0.30$
    - $\Gamma_{J1809} = 1.70 \pm 0.10$
- this highlights an unexpected MHD phenomenon!

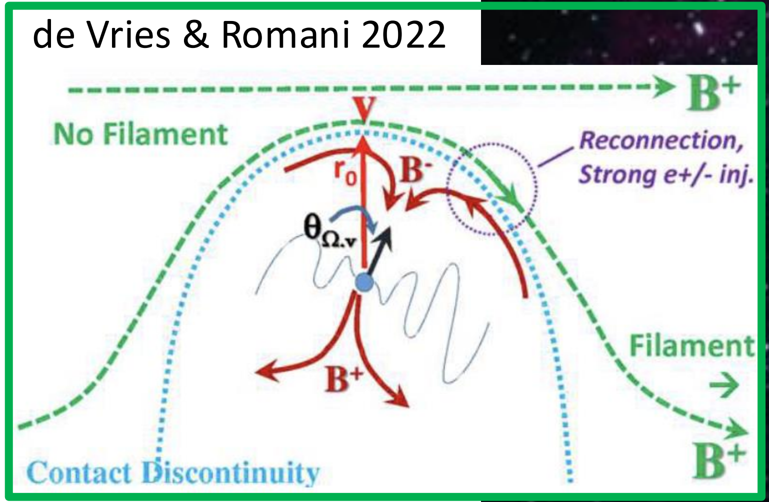
de Vries & Romani 2022

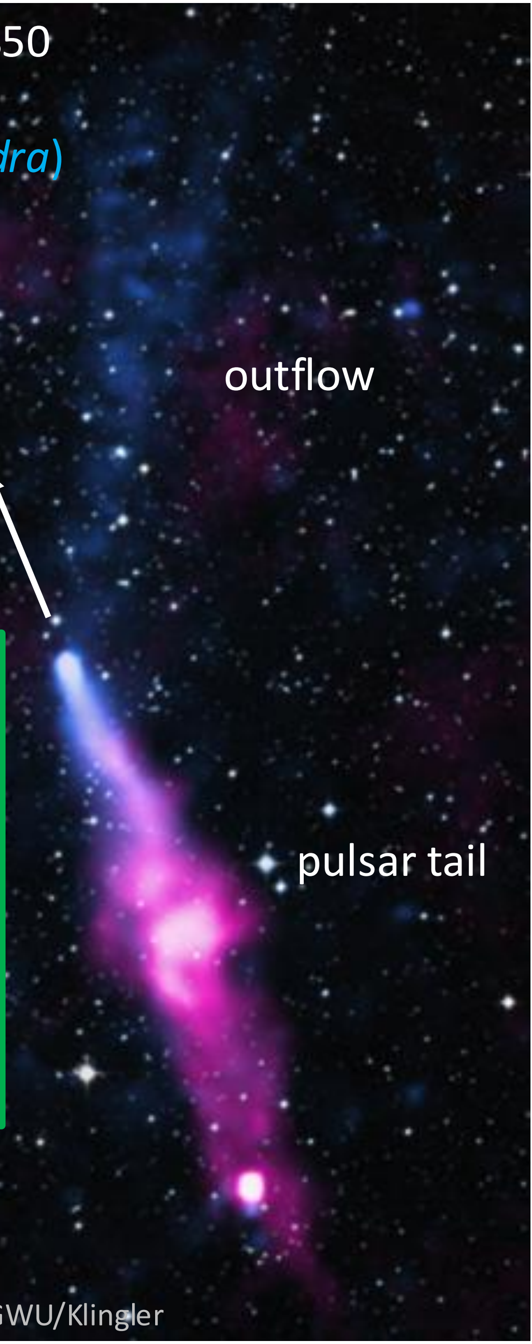

Image: NASA/CXC/GWU/Klingler

Multiwavelength Spectra

- PWN/tail seen in radio, so its spectrum is well-constrained
- The misaligned outflow, however, is not.
- Next steps: propose IR observations to constrain lower-energy outflow spectrum → constrain minimum injected particle energy
- This will inform us about the particle escape mechanism

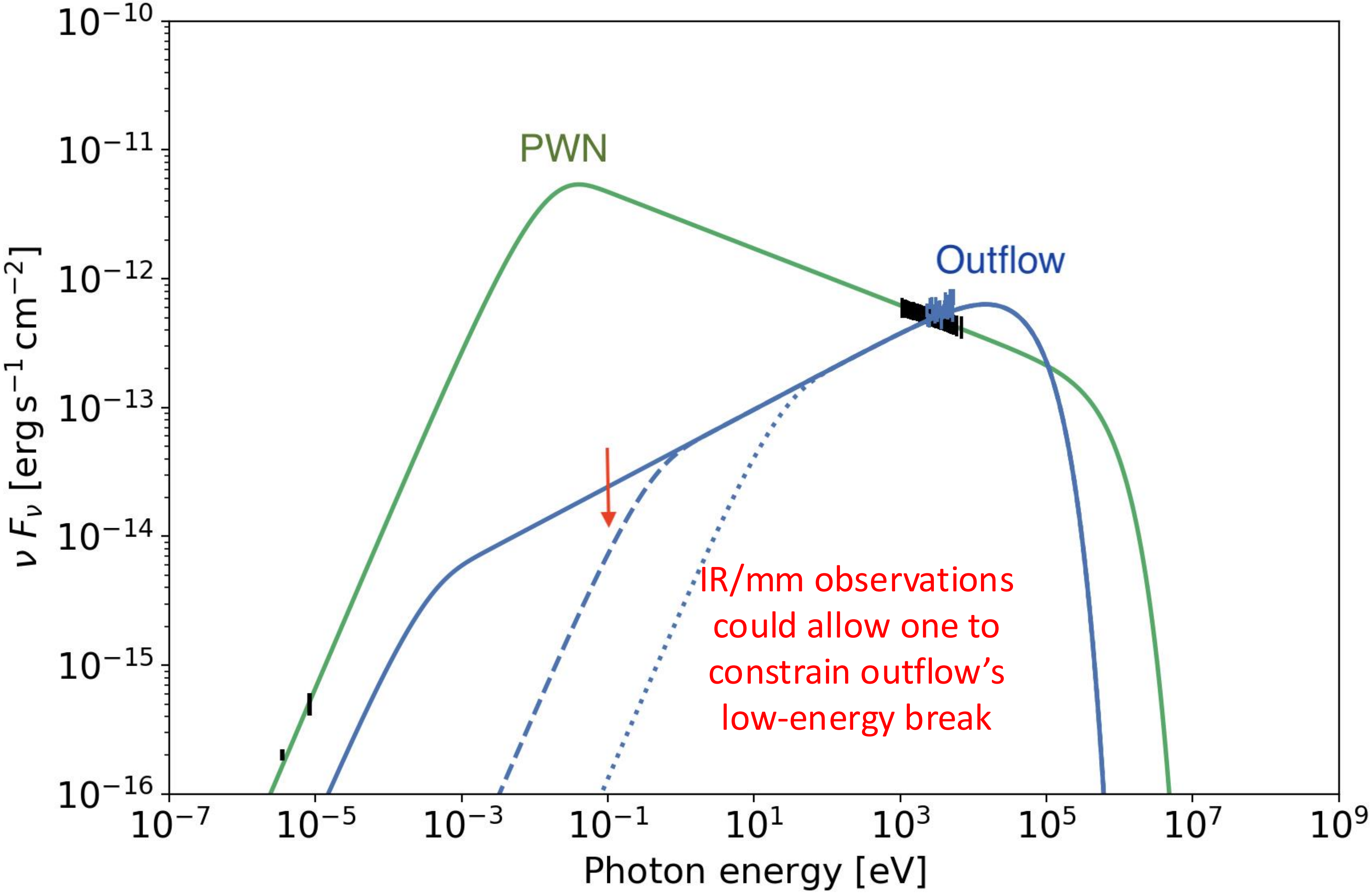

IR/mm observations could allow one to constrain outflow's low-energy break

NUSTAR Observations

Hard X-ray spectra provide evidence of spectral cooling along the filament

- $\Gamma_1 = 1.71 \pm 0.04$
- $\Gamma_2 = 1.86 \pm 0.05$
- $\Gamma_3 = 1.74 \pm 0.04$

0.5-8 keV

$\Gamma_1 = 1.79 \pm 0.08$

$\Gamma_2 = 2.03 \pm 0.09$

$\Gamma_3 = 2.21 \pm 0.08$

3-79 keV

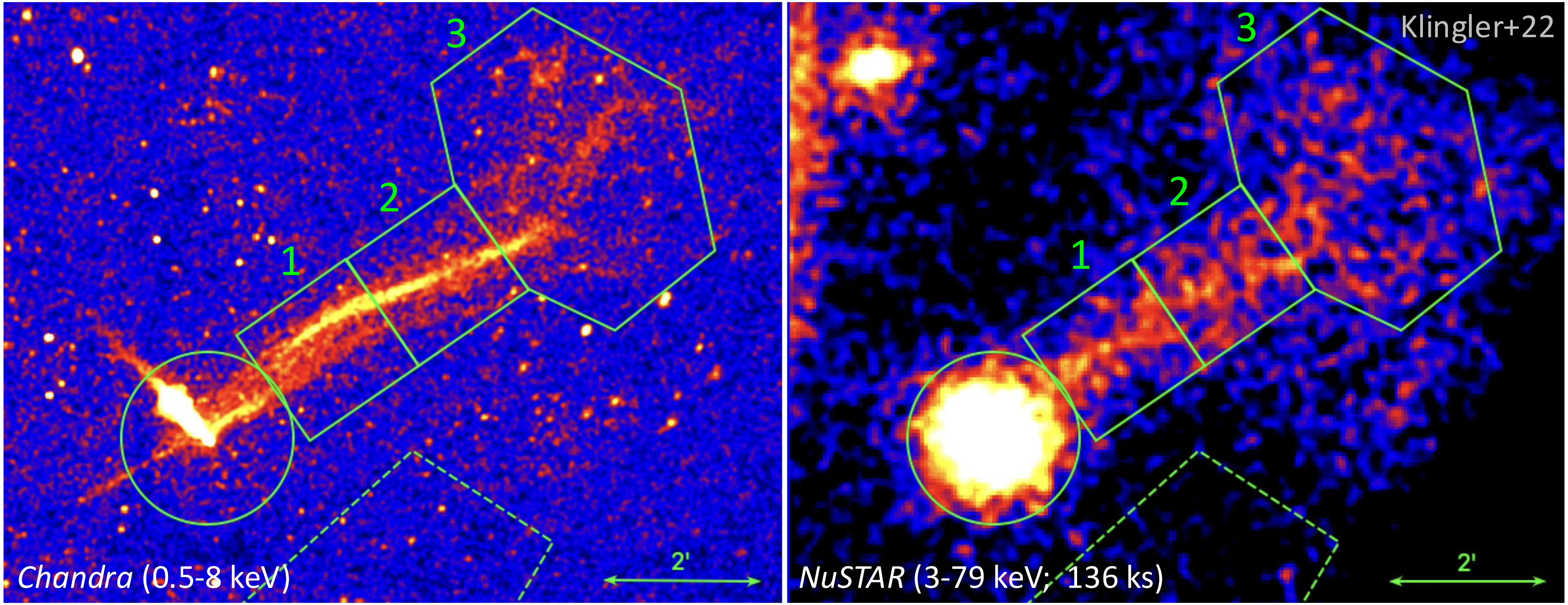

More highly-supersonic PWNe with misaligned outflows

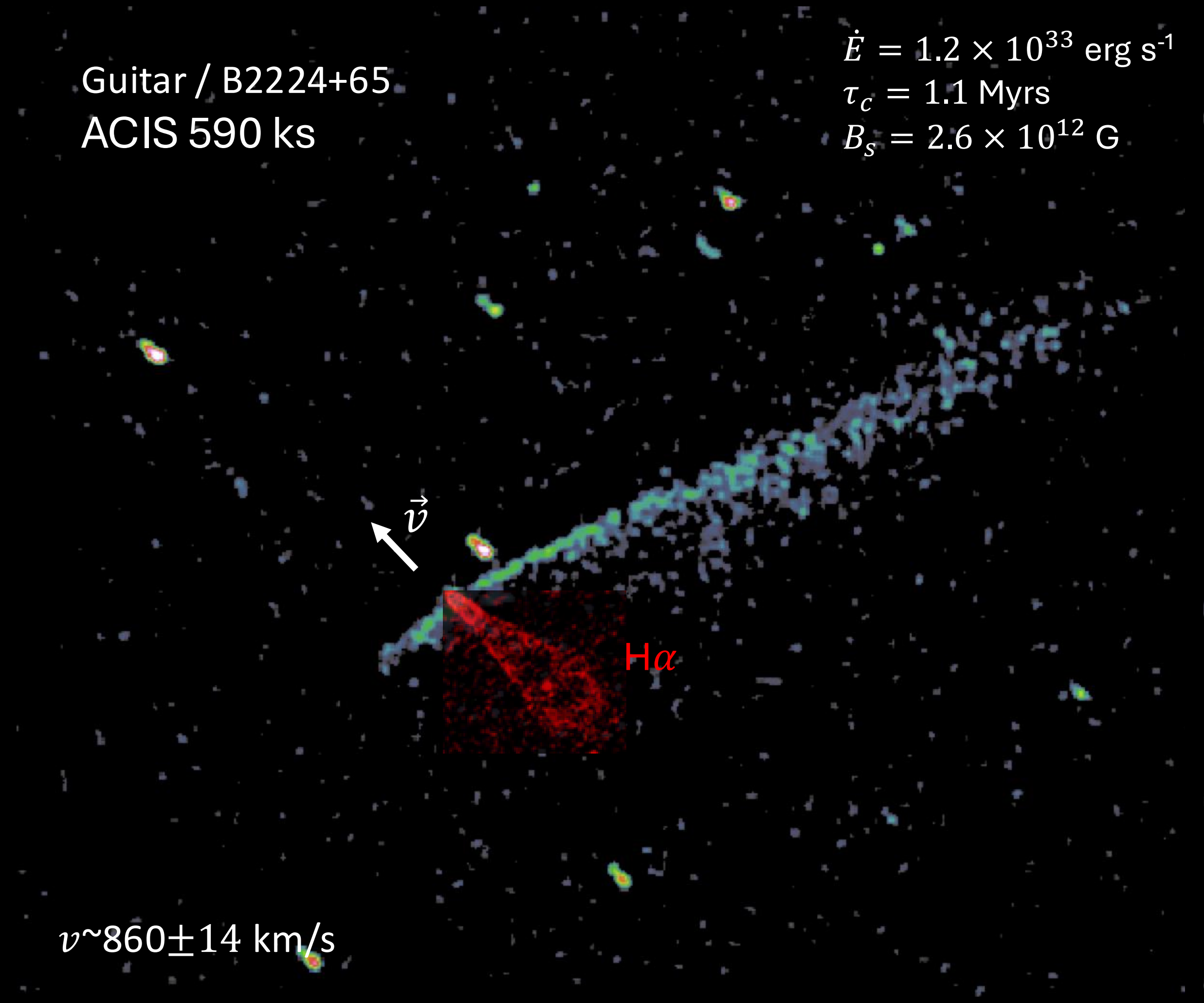

Guitar / B2224+65
ACIS 590 ks

$\dot{E} = 1.2 \times 10^{33}$ erg s^{-1}
$\tau_c = 1.1$ Myrs
$B_s = 2.6 \times 10^{12}$ G

v~860±14 km/s

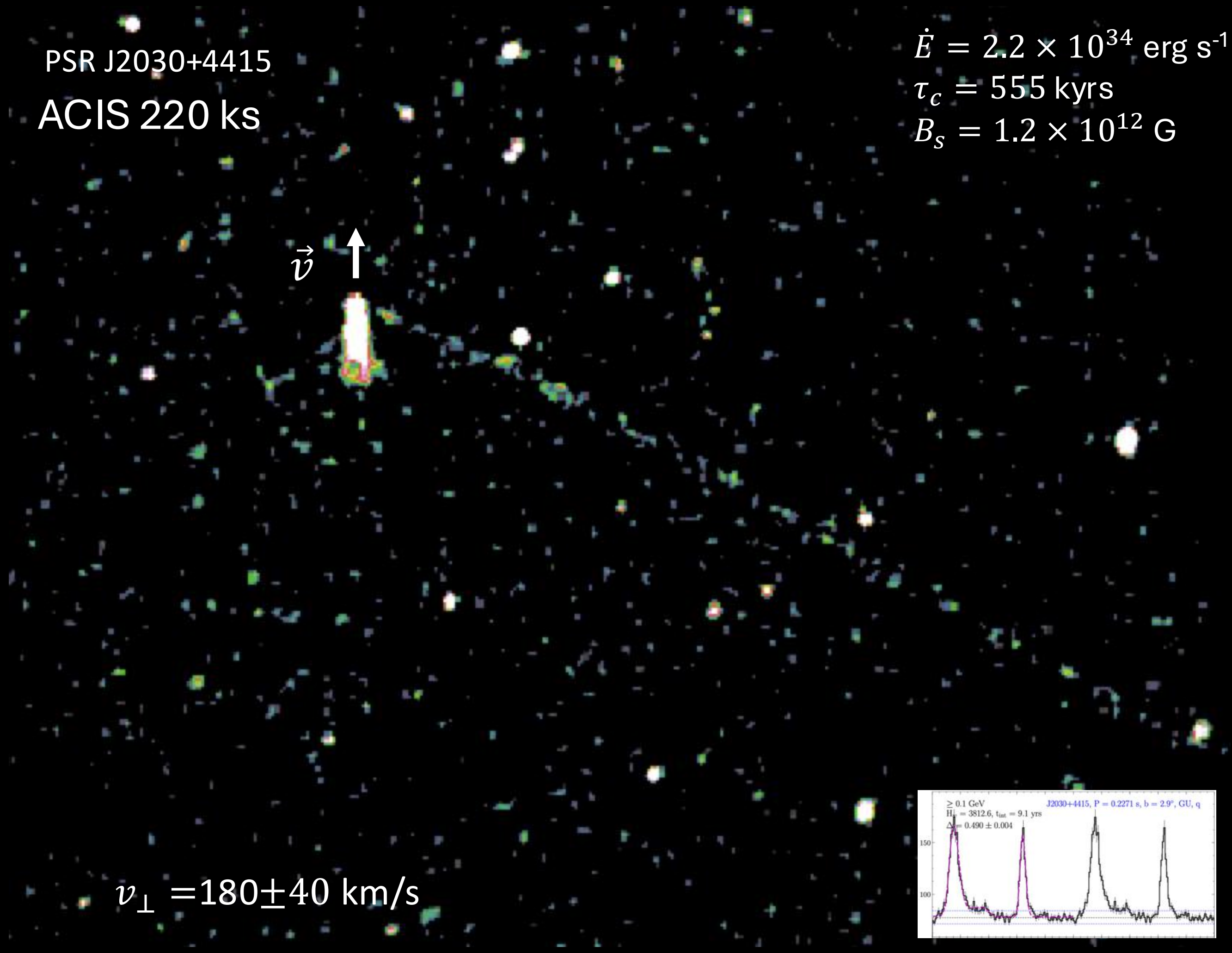

PSR J2030+4415
ACIS 220 ks

$\dot{E} = 2.2 \times 10^{34}$ erg s^{-1}
$\tau_c = 555$ kyrs
$B_s = 1.2 \times 10^{12}$ G

$v_\perp$ =180±40 km/s

For more of these see Dinsmore & Romani (2024) and Dinsmore & Romani (2026)

PXF's with NewAthena

Barret+ 2022

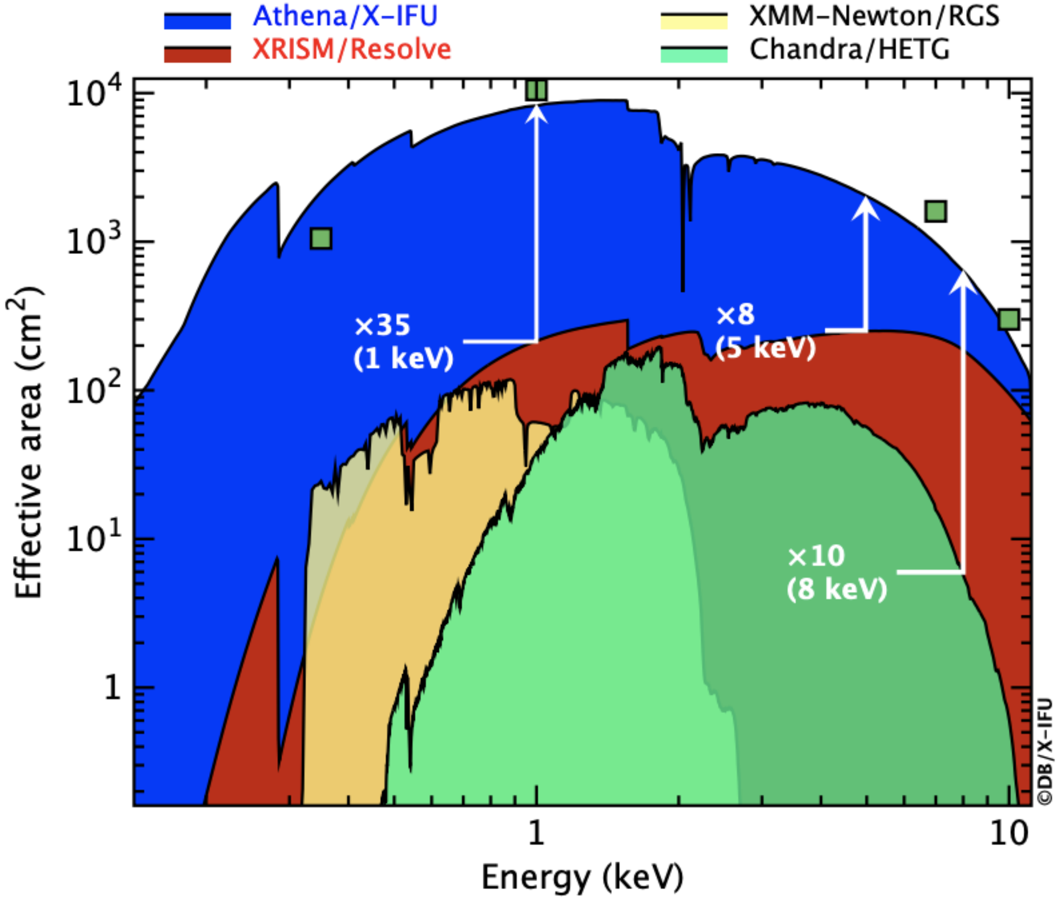

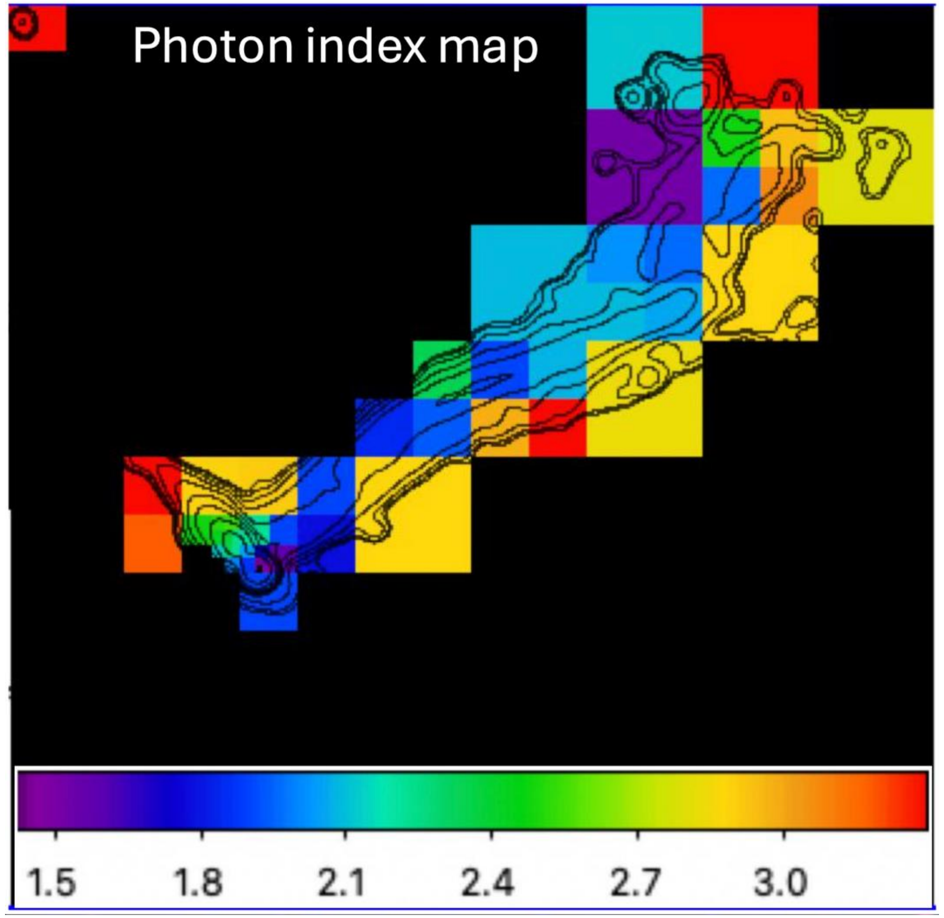

Conclusion

- What does asymmetry tell us and why some supersonic PWNe are missing PFs?
- Could the PF particles come from ISM electron (not pulsar wind e^+e^-) begin accelerated in colliding flows (Bykov et al. 2017)?
- PF’s help us learn about the ISM magnetic field structure and strength
- NewAthena can help to constrain the spatial evolution of the spectra in PF’s

Backup slides

Fine Structure of the Pulsar Filament

- deep Chandra image reveals a patter of parallel arcsecond-scale ”threads” within the PF.
- could indicate variations in reconnection of PWN field with the external (ISM) magnetic field, sampled as the pulsar travels through an inhomogeneous ISM
  - as pulsar moves through ISM of varying density, the bow shock stand-off distance would fluctuate, causing changes in the numbers and energies of particles escaping
- PF’s are symmetric on very small scales
- There is emission ahead of pulsar, beyond the standoff distance

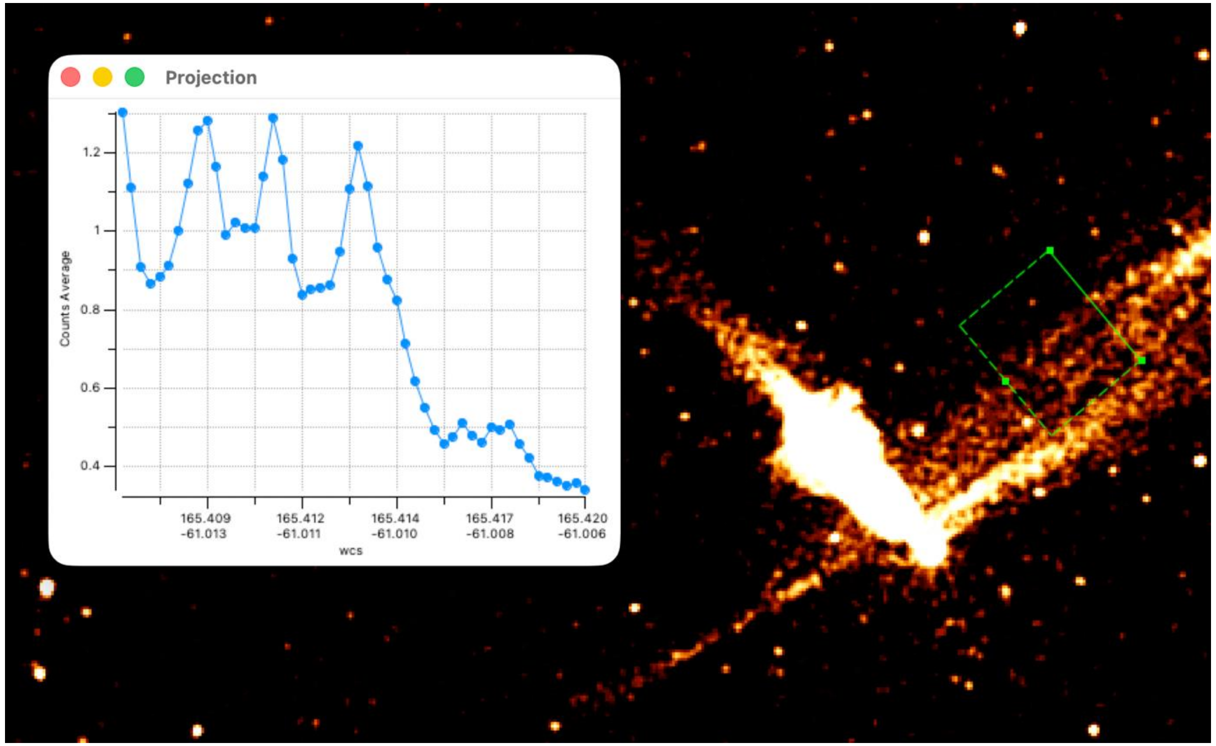

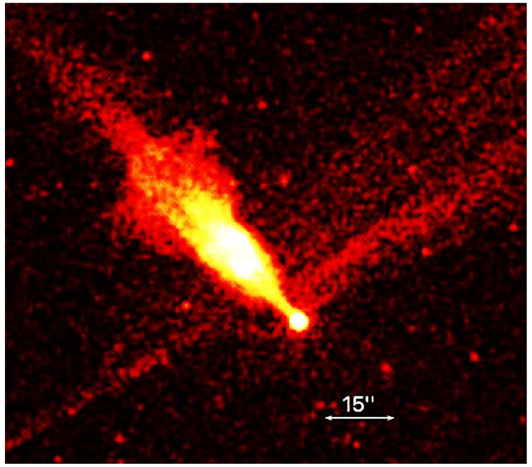

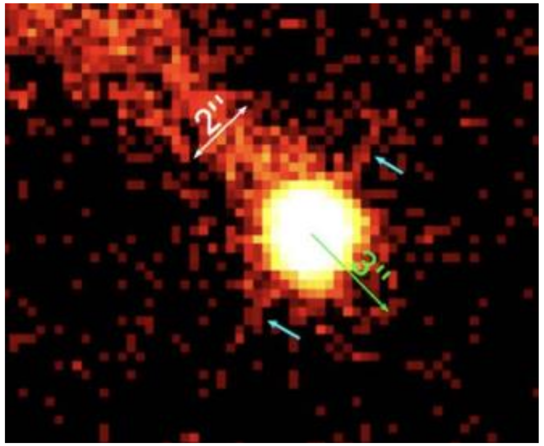

PIC simulations of instabilities

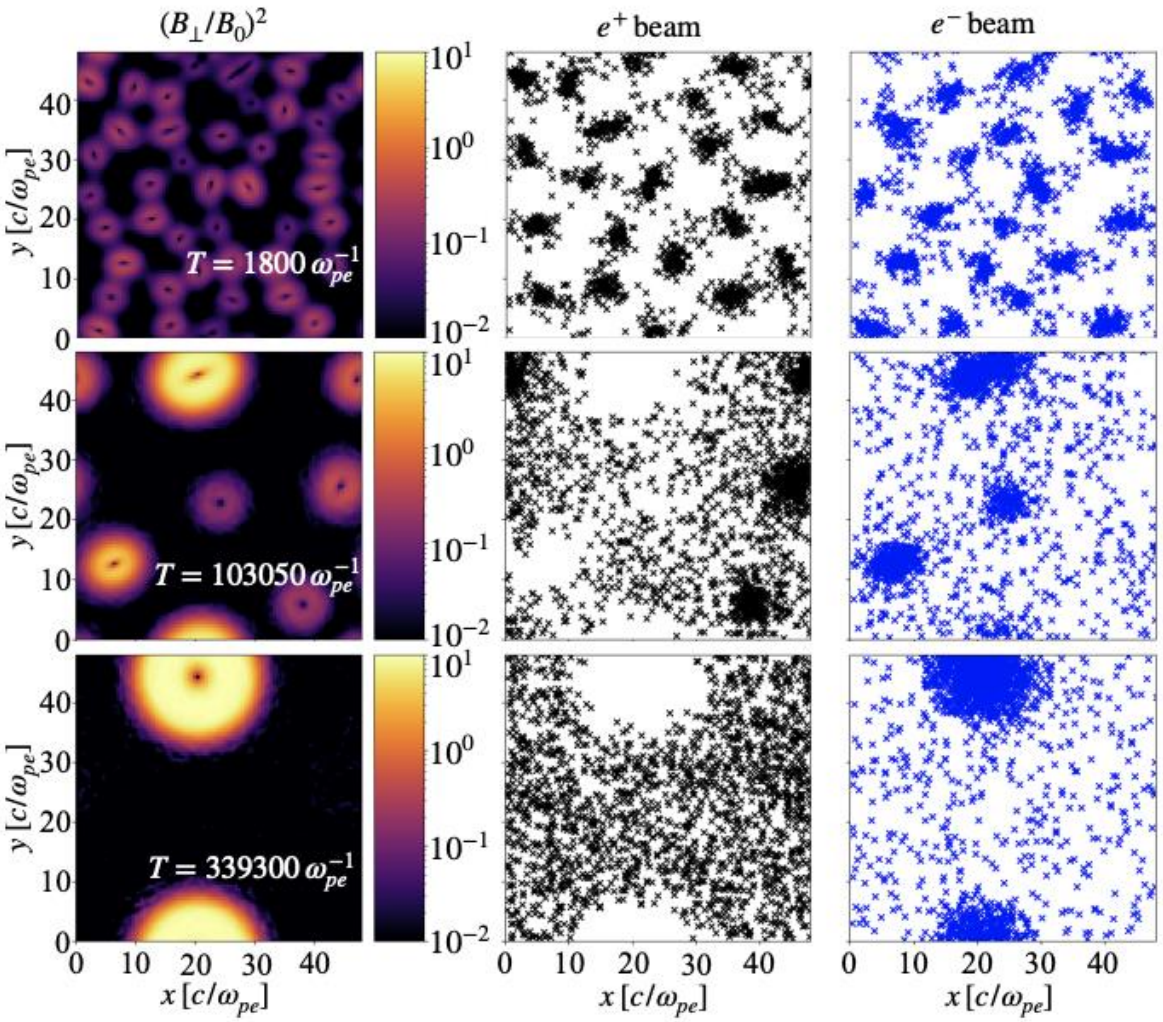

Orusa & Sironi (2026)

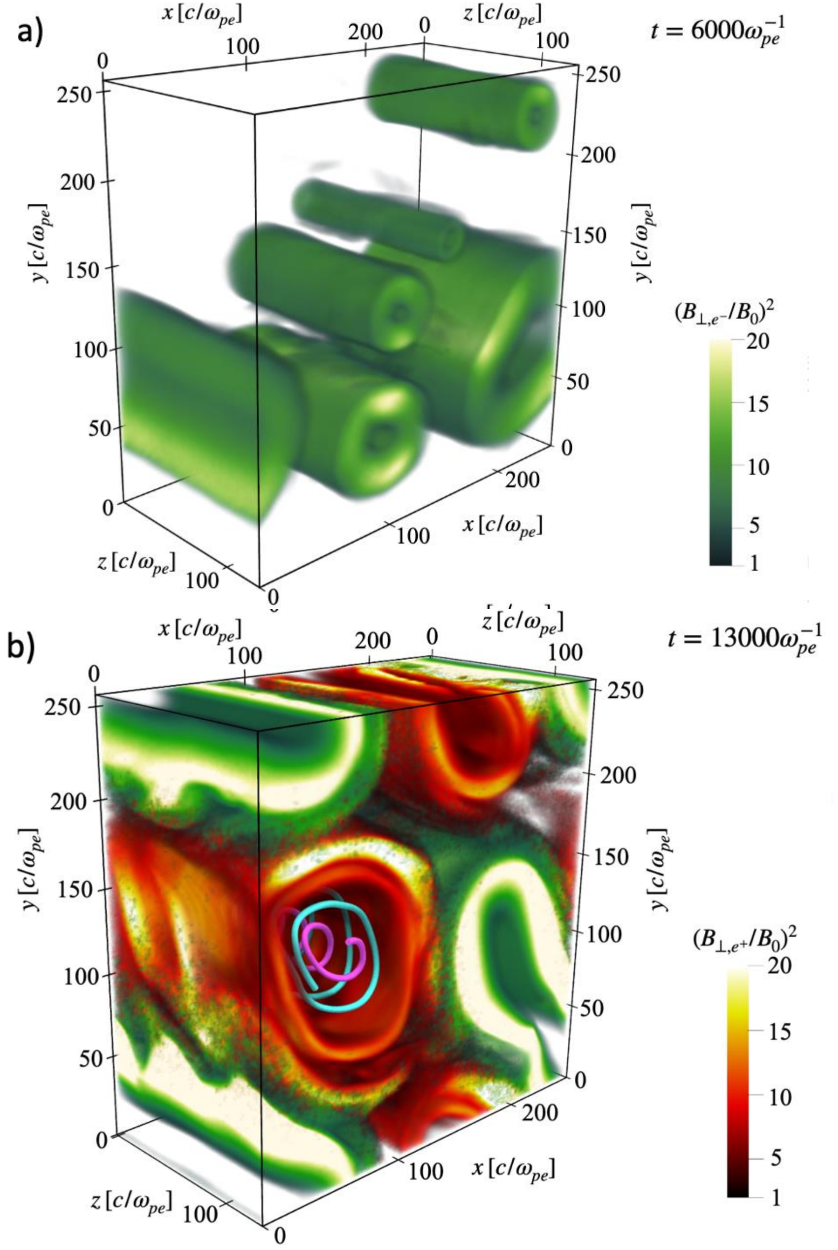

- Pulsar wind particles with gyroradii $r_g(E) > r_0$ can escape into ISM, where

$$r_0 = 0.13'' \left(\frac{\mu}{33\ \mathrm{mas/yr}}\right)^{-1/2} \left(\frac{d}{6.3\ \mathrm{kpc}}\right)^{-2} n\,(\sin i)^{-1}$$

is the bow shock stand-off distance

- The synchrotron emission can only be expected above

$$E_c \sim 1(B_{ISM}/5\ \mu G)^3\ (\mu/15\ \mathrm{mas\ yr}^{-1})^2\ (d/7\ \mathrm{kpc})^{-2} nH^{-1}\ \mathrm{keV}$$

because particles emitting synchrotron radiation at lower energies should not be escaping

- From observed synchrotron emission escaping particle energies: $E_{esc} \gtrsim 0.3\ \mathrm{PeV}\left(\frac{\epsilon}{8\ \mathrm{keV}}\right)^{1/2}\left(\frac{B_{PF}}{5\ \mu G}\right)^{-1/2}$
- If the transverse angular size of the structure is δ, then confinement requires: $\mathrm{B} \gtrsim 13\mu\mathrm{G}\left(\frac{\epsilon}{8\ \mathrm{keV}}\right)^{1/3}\left(\frac{\delta}{0.5''}\right)^{-2/3}\left(\frac{d}{6.3\ kpc}\right)^{-2/3}$
- For comparison, the maximum energy from potential drop across the polar cap: $E_{max} \sim \left(\frac{\dot{E}}{c}\right)^{1/2} = 1.7\left(\frac{\dot{E}}{10^{36}\ \mathrm{erg\ s^{-1}}}\right)^{1/2}$ PeV
- For Lighthouse's $\dot{E} = 1.4 \times 10^{36}$ erg/s, $E_{max} \sim 2\ \mathrm{PeV}$, hence, strong amplification of magnetic field inside the pulsar filament is not required but can happen in some parts of it.
- The situation is different, however, for the Guitar nebula filament where $\dot{E} = 1.3 \times 10^{33}$ erg/s and $E_{esc} > E_{max}$ if B_{PF}= 5 μG .

Inferring PF Properties

- studying PFs can tell us about ISM properties
  - with the measured broad-band spectra, we can estimate the magnetic field across the outflow (i.e., the ISM):

$$B = \left[\frac{L(\nu_m, \nu_M)\sigma}{\mathcal{A}V} \frac{\Gamma - 2}{\Gamma - 1.5} \frac{\nu_1^{1.5-\Gamma} - \nu_2^{1.5-\Gamma}}{\nu_m^{2-\Gamma} - \nu_M^{2-\Gamma}} \right]^{2/7}$$

    - $B_1 \sim 6\ \mu\mathrm{G}$
    - $B_2 \sim 6\ \mu\mathrm{G}$
    - $B_3 \sim 4\ \mu\mathrm{G}$
  - provides an independent but consistent check of $B_{\mathrm{ISM}} \sim 5\ \mu\mathrm{G}$ estimated through other ways (Ferriere 2015)
  - shows that ISM B-fields remain aligned up to scales > 16 pc
- escaped pulsar wind properties:

$$t_{\mathrm{syn}} \sim 1000(E_{\mathrm{syn}}/25\ \mathrm{keV})^{-1/2}(B/5\ \mu\mathrm{G})^{-3/2}\ \mathrm{yr}$$

$$\gamma \sim 3 \times 10^8 (E_{\mathrm{syn}}/8\ \mathrm{keV})^{1/2}(B/5\ \mu\mathrm{G})^{-1/2}$$

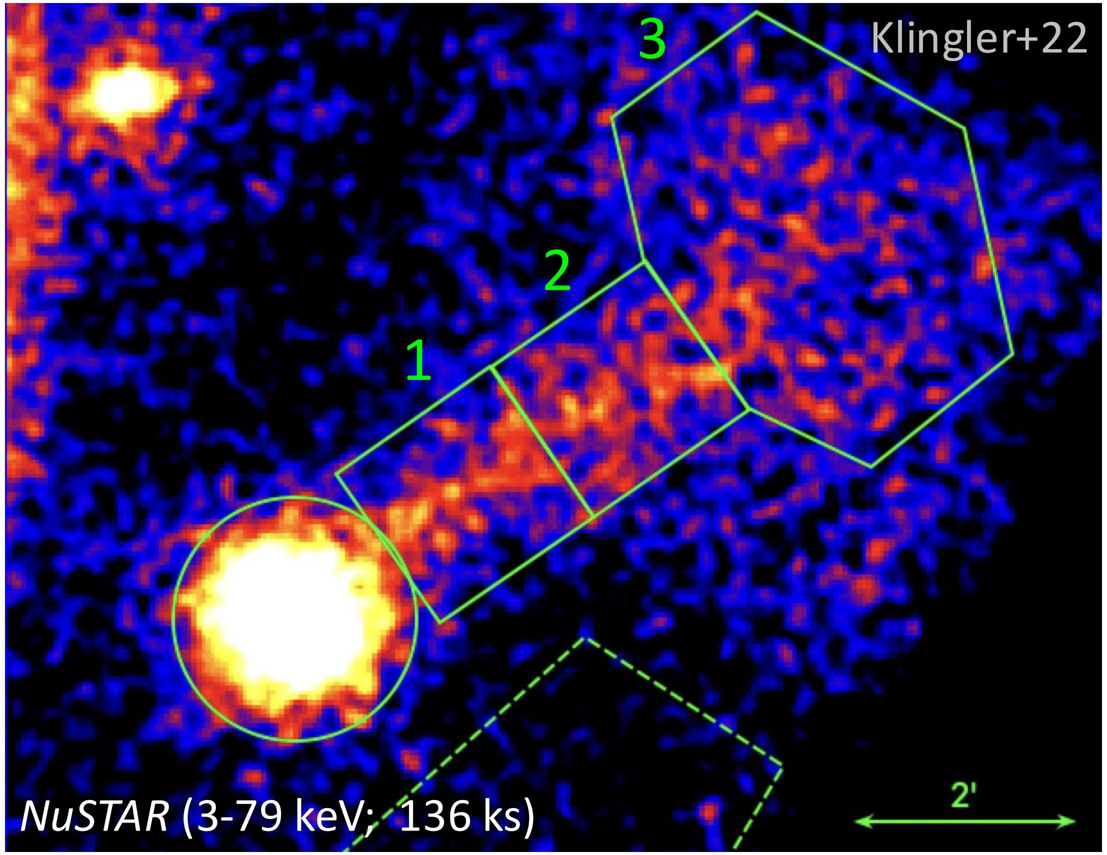

Klingler+22

NuSTAR (3-79 keV; 136 ks)

Theory: Reconnection between PWN and ISM fields

(Barkov, Lyutikov, Klingler, & Bordas 2019)

de Vries & Romani 2022

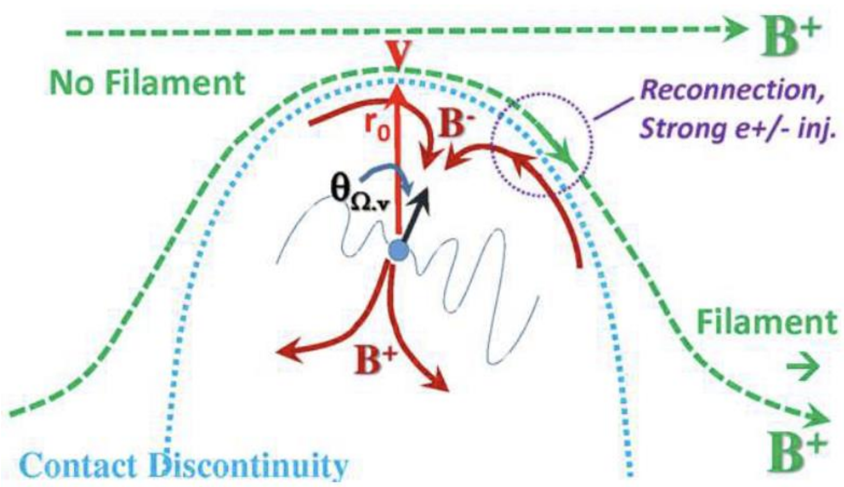

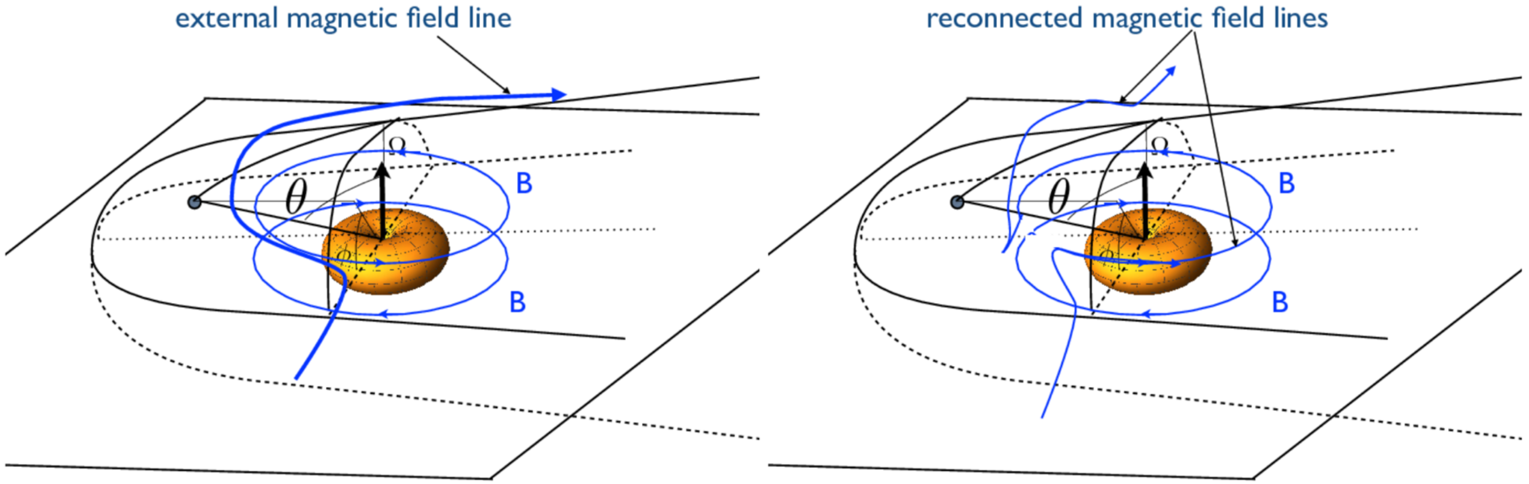

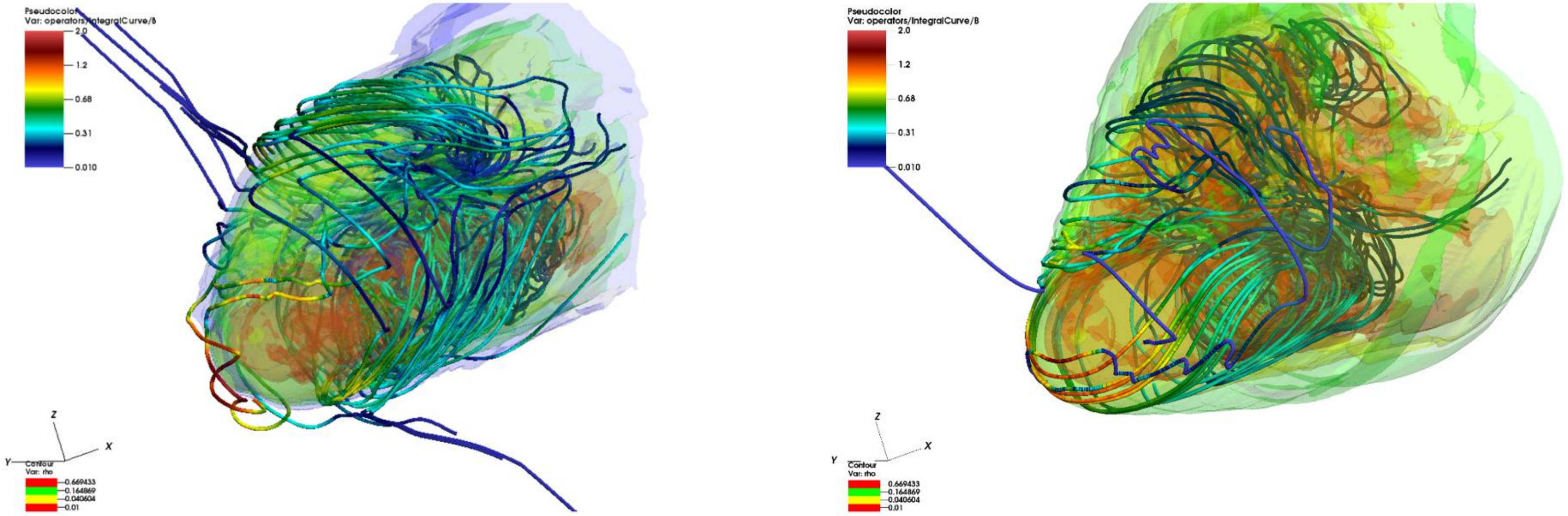

Figure 8. Iso-density surfaces and velocity vectors for the slow model (left) and fast one (right).

More examples of MAOs? But these show some evidence of bending with increasing distance from pulsar which one can expect form “fluid” jets…

MSH 15-56 PWN (see Temim, T., et al. 2017)

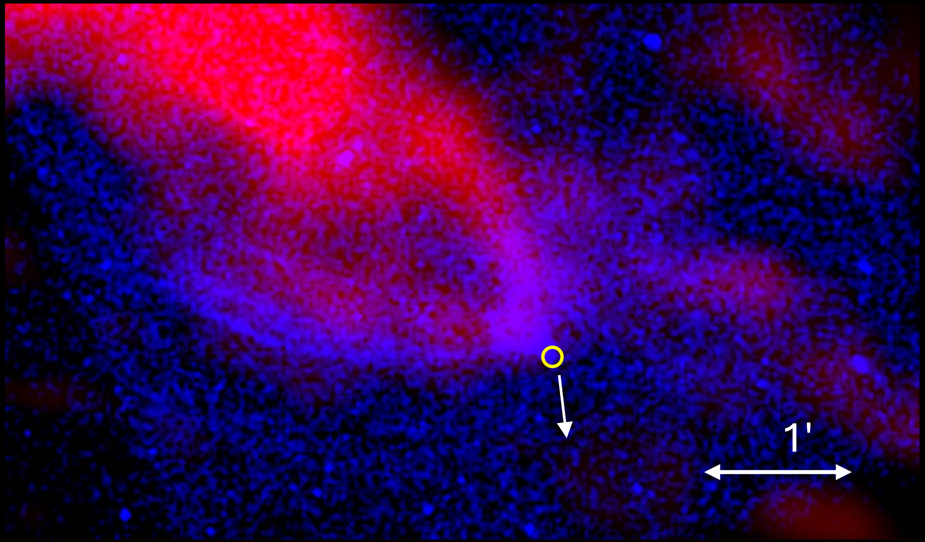

Tadpole (Klingler et al. 2020)

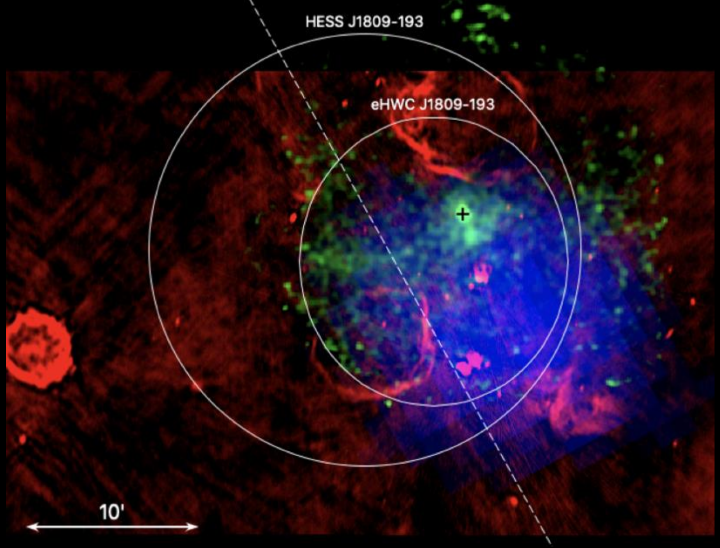

Dragonfly (Van Etten et al. 2008)

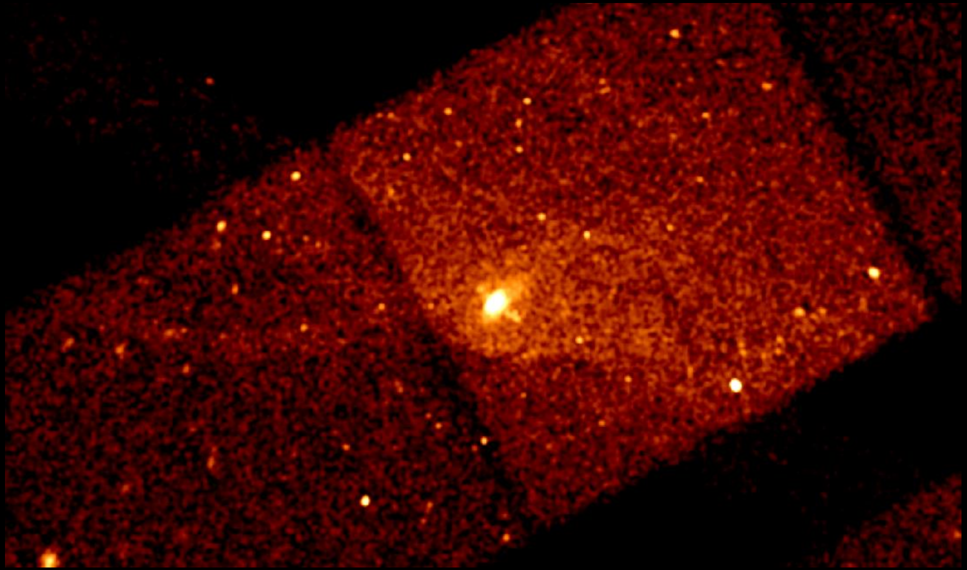

CTA1 (Gagnon et al. in prep.)

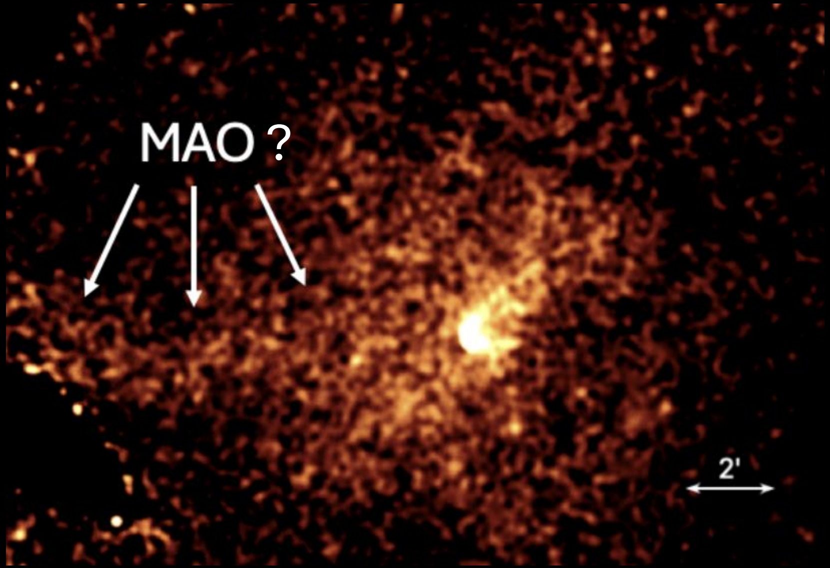

Constraints on particle energies

If the particles are indeed escaping and moving in a typical ISM field, one can use standard synchrotron estimate to estimate Lorentz factors, $\gamma_{\rm esc}$, the escaped electrons (Bandiera 2008):

$$\gamma_{\rm esc} \gtrsim 6 \times 10^8 (\epsilon/8\,{\rm keV})^{1/2} (B_{\rm ISM}/5\,\mu{\rm G})^{-1/2}$$

This scaling assumes no $B_{\rm ISM}$ amplification!

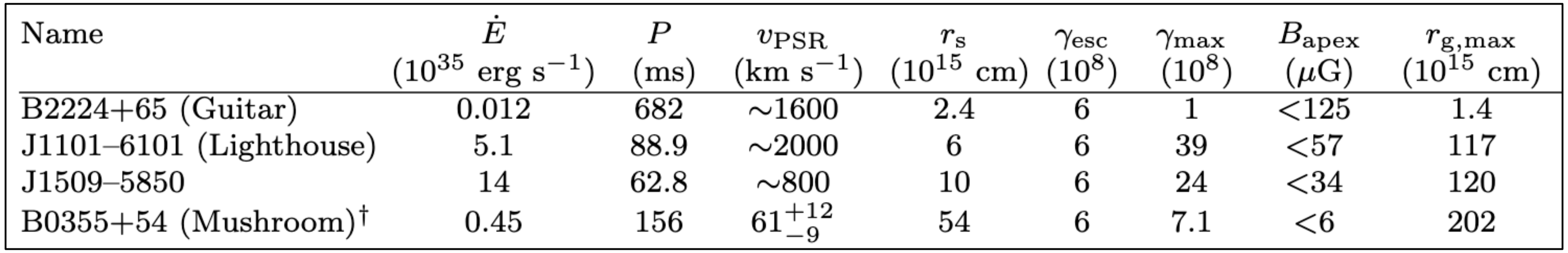

Name	$\dot{E}$ (10^{35} erg s^{-1})	P (ms)	$v_{\rm PSR}$ (km s^{-1})	$r_{\rm s}$ (10^{15} cm)	$\gamma_{\rm esc}$ (10^8)	$\gamma_{\rm max}$ (10^8)	$B_{\rm apex}$ (μG)	$r_{\rm g,max}$ (10^{15} cm)
B2224+65 (Guitar)	0.012	682	$\sim$1600	2.4	6	1	<125	1.4
J1101–6101 (Lighthouse)	5.1	88.9	$\sim$2000	6	6	39	<57	117
J1509–5850	14	62.8	$\sim$800	10	6	24	<34	120
B0355+54 (Mushroom)†	0.45	156	61^{+12}_{-9}	54	6	7.1	<6	202

$$\gamma_{\rm max} \sim \Phi e/m_e c^2 \sim 1 \times 10^{10} (\dot{E}/10^{37}\ {\rm erg/s})^{1/2}$$

Potential drop across PC:

$$\Phi \sim (\dot{E}/c)^{1/2}$$

From the escape condition, $r_g \gtrsim r_{\rm s}$,

one can also estimate the magnetic field within the apex region of the PWN

$$B_{\rm apex} \lesssim 34 (\epsilon/1\,{\rm keV})^{1/2} (B_{\rm ISM}/5\,\mu{\rm G})^{-1/2} (r_{\rm s}/10^{16}\ {\rm cm})^{-1}\ \mu{\rm G}$$

Radio-bright (X-ray faint) misaligned outflow?

PSR J0538+2817

X-ray: CXO, 93 ks

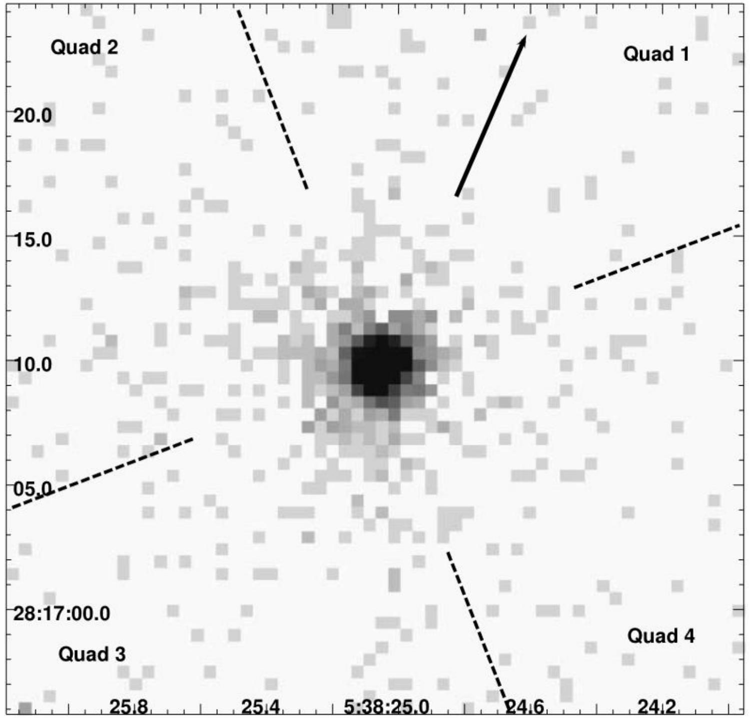

FIG. 2.—ACIS-I 0.5–8 keV image. The arrow indicates the pulsar's proper motion direction in its LSR. The dashed lines separate the four quadrants used to measure the azimuthal distribution of the extended emission.

Ng et al. 2007

Radio: RACS 890-1300 MHz

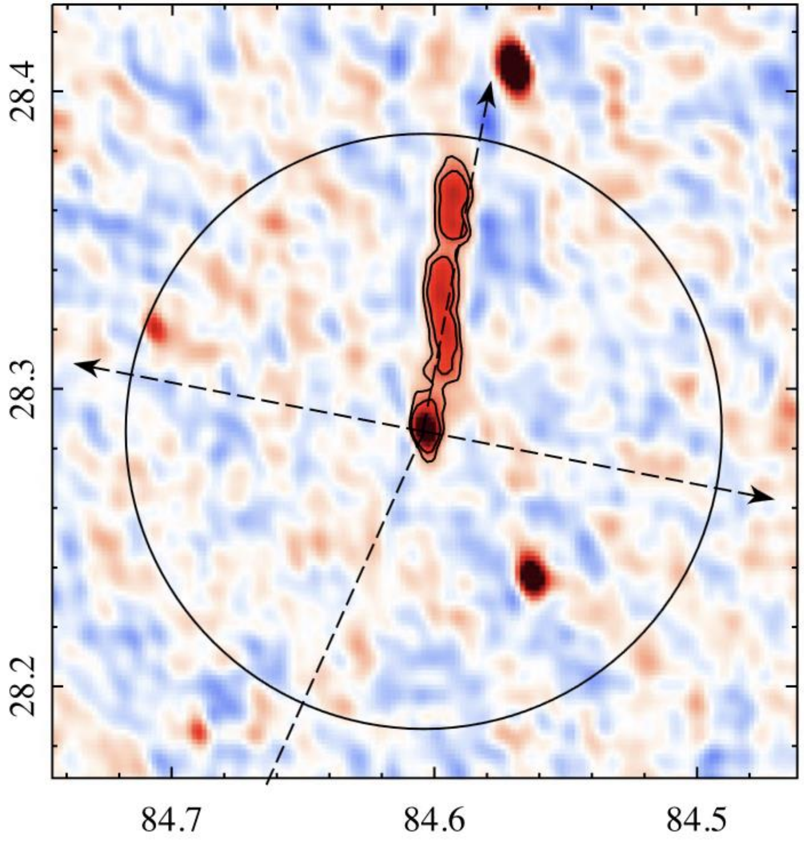

Khabibullin et al. 2024

Misaligned outflows: tend to have hard spectra

Emission is also seen in harder X-rays (with some evidence for mild cooling with distance). The length of the structure is about 7-8 arcmin (13-16 pc).

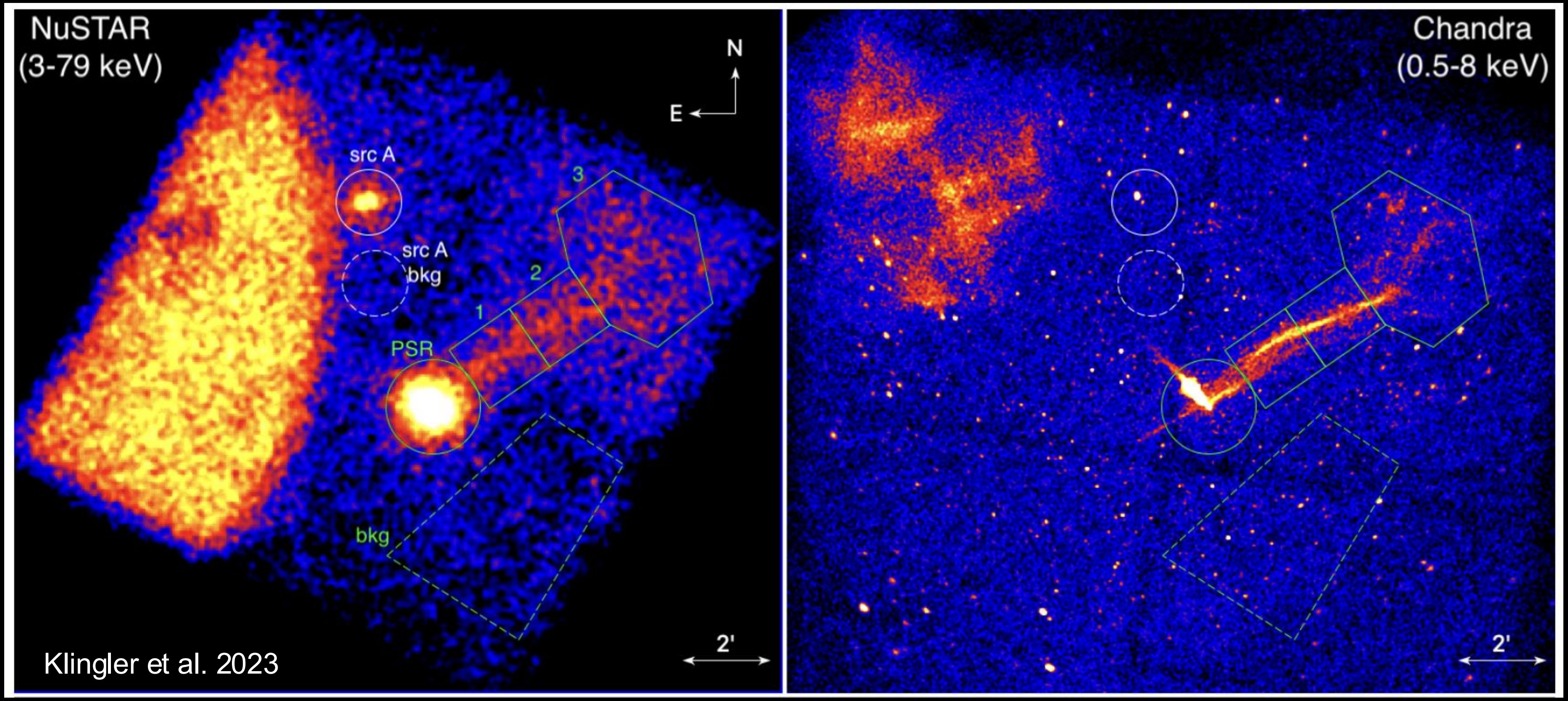

Klingler et al. 2023

This implies rapid diffusion of particles along the ISM B-field that must remain relatively straight over the visible extent of the structure. Transverse (to the feature) diffusion must be much slower (Bohm?).

Theory: 3D dynamics and morphology of bow-shock PWNe

Barkov, Lyutikov, & Khangulyan (2019)

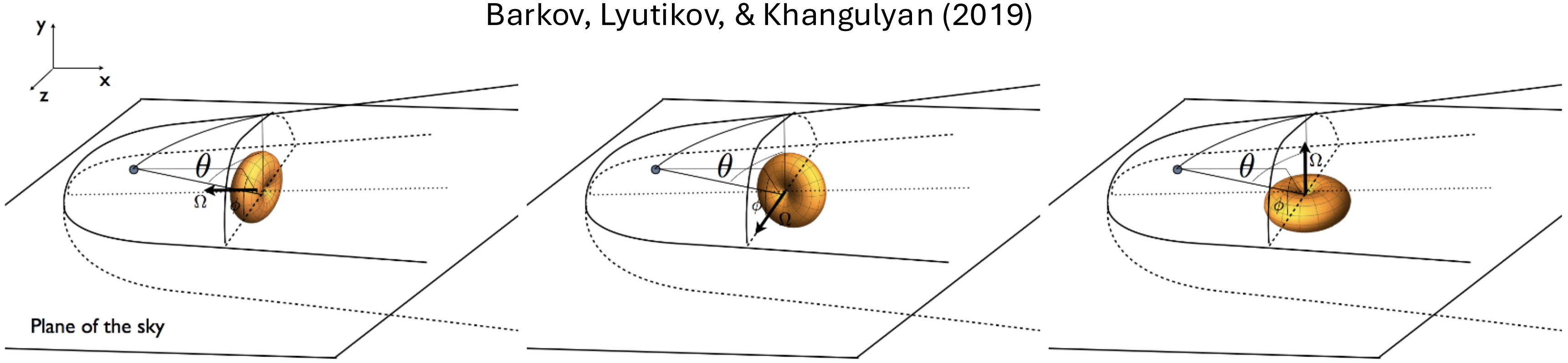

Figure 7. Basic geometries: rifle-bullet (with the spin of the NS aligned with the velocity), frisbee (with the spin of the NS perpendicular to the velocity but lying in the plane of the sky), and cart-wheel (with the spin of the NS perpendicular both to the velocity and the plane of the sky). The central doughnut-like structure indicates the distribution of wind power, $\propto \sin^2\theta_p$, where θ_p is the polar angle; θ is a polar angle with respect to the velocity.

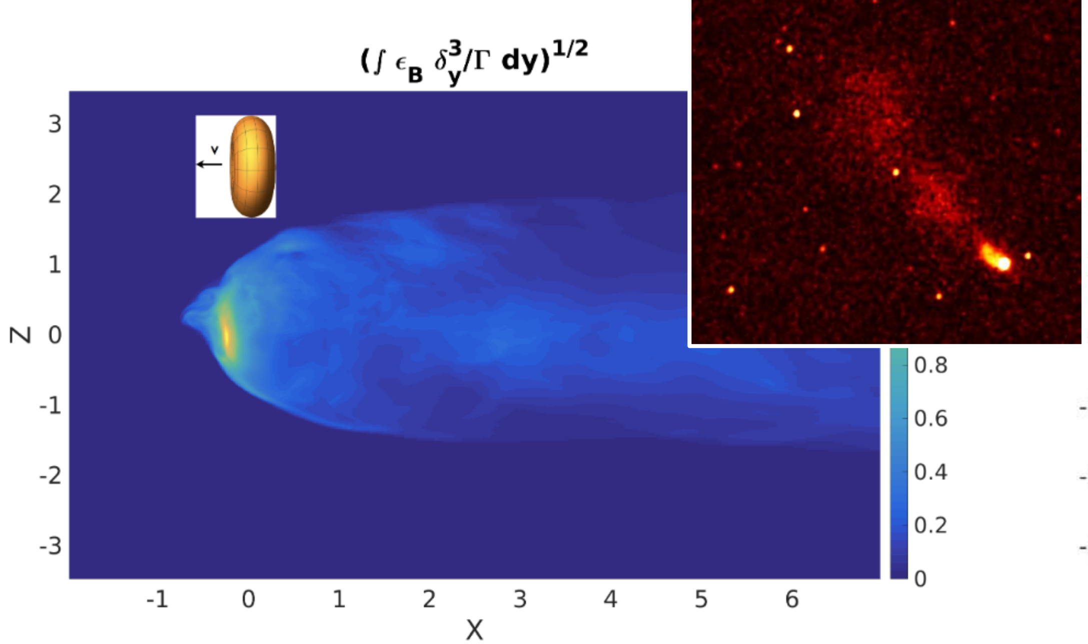

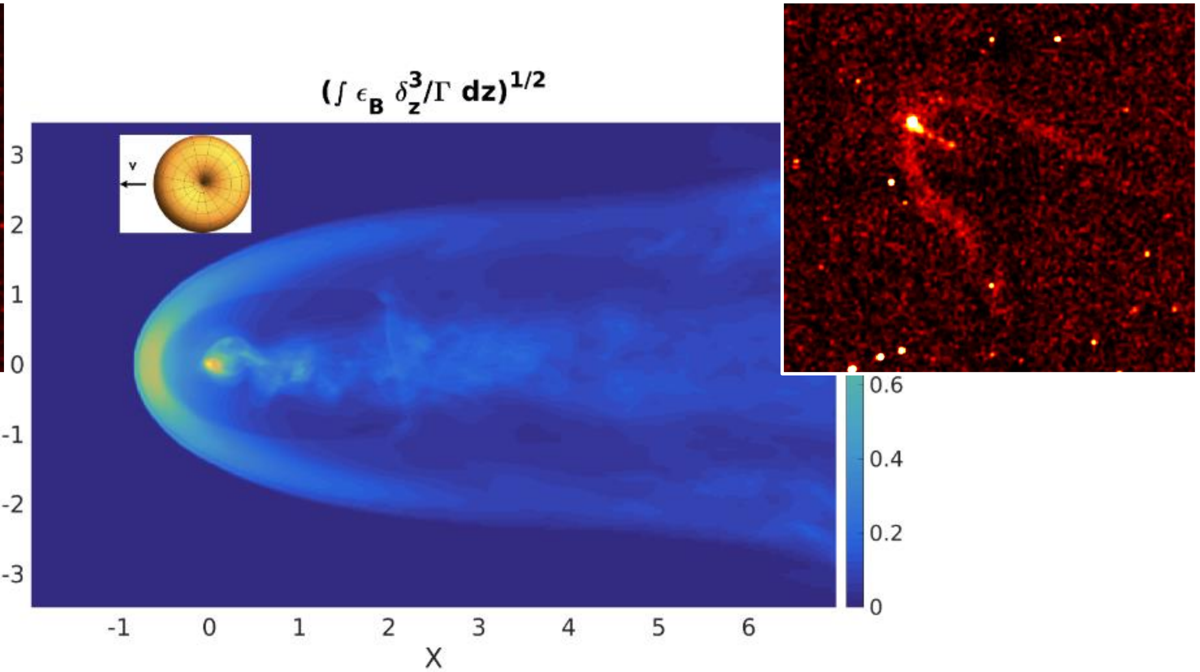

Highly Supersonic PWNe

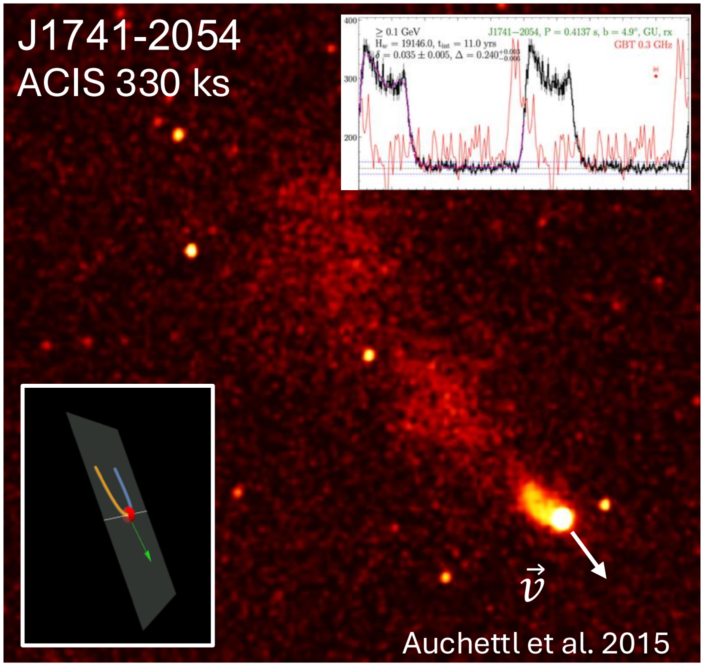
J1741-2054
ACIS 330 ks

Auchettl et al. 2015

$\dot{E} = 9.5 \times 10^{33}$ erg s^{-1}
$\tau_c = 386$ kyrs
$B_s = 2.7 \times 10^{12}$ G

No good radio images yet

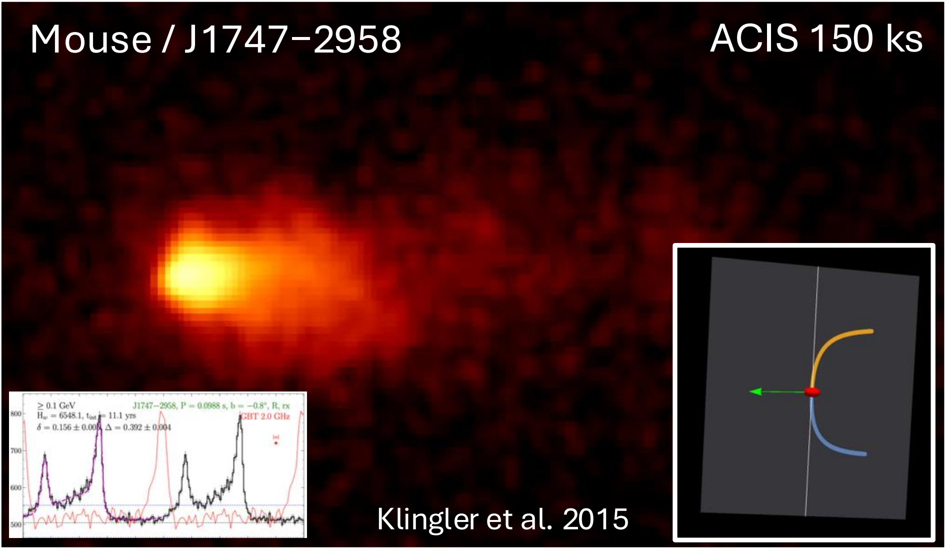
Mouse / J1747−2958
ACIS 150 ks

Klingler et al. 2015

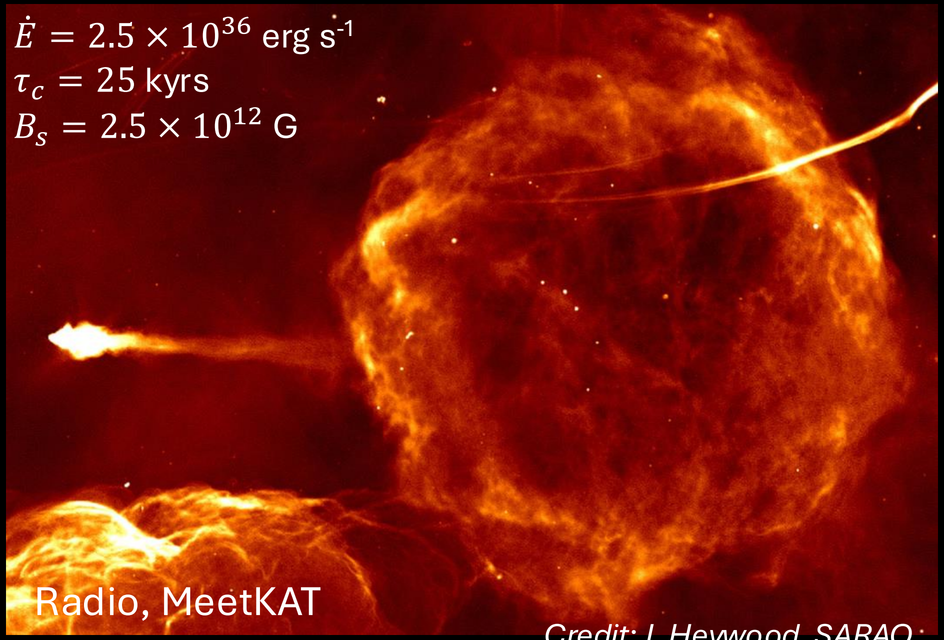
$\dot{E} = 2.5 \times 10^{36}$ erg s^{-1}
$\tau_c = 25$ kyrs
$B_s = 2.5 \times 10^{12}$ G

Radio, MeetKAT

Credit: I. Heywood, SARAO

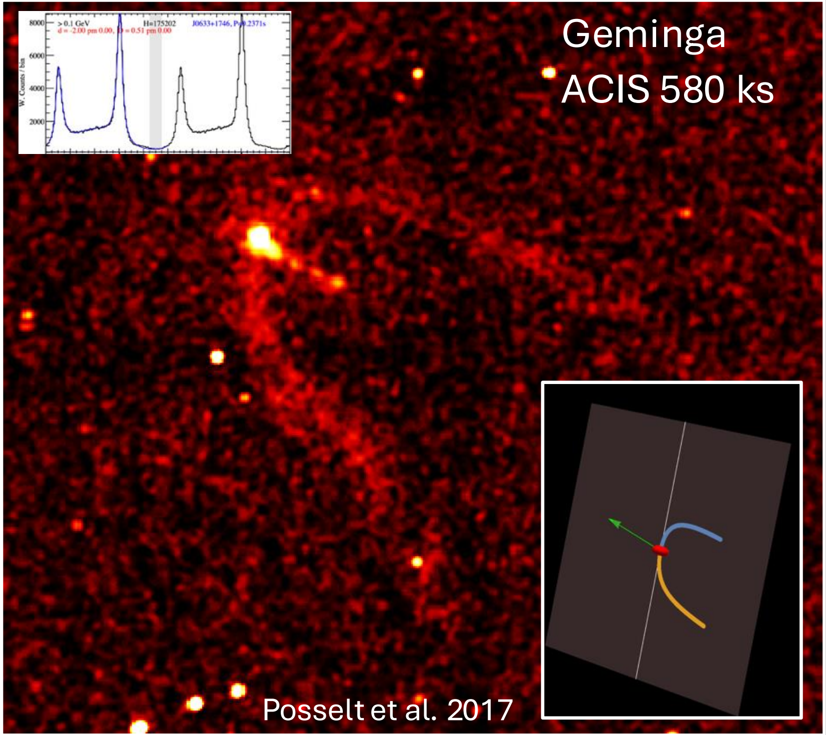
Geminga
ACIS 580 ks

Posselt et al. 2017

$\dot{E} = 3.2 \times 10^{34}$ erg s^{-1}
$\tau_c = 342$ kyrs
$B_s = 1.6 \times 10^{12}$ G

No good radio images yet

Comparison with Other Misaligned Outflows

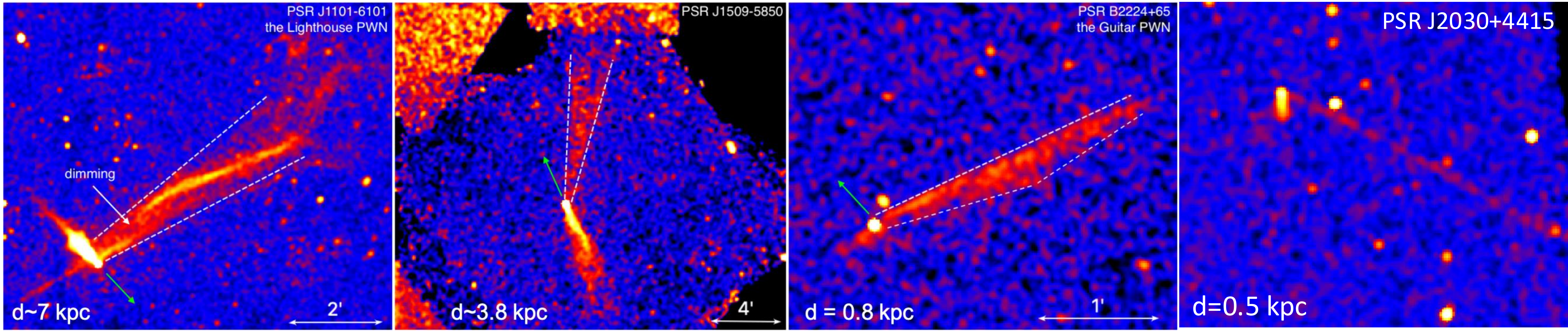

- open questions remain: what factors cause observed differences?
  - conical (widening) vs collimated
  - threads?
  - lack of tail (in the Guitar PWN)
- future detections in IR and in MeV/GeV/TeV can place constraints on min/max particle energies via multiwavelength modeling
- plenty of theoretical/observational work to be done!

Pulsar Filaments

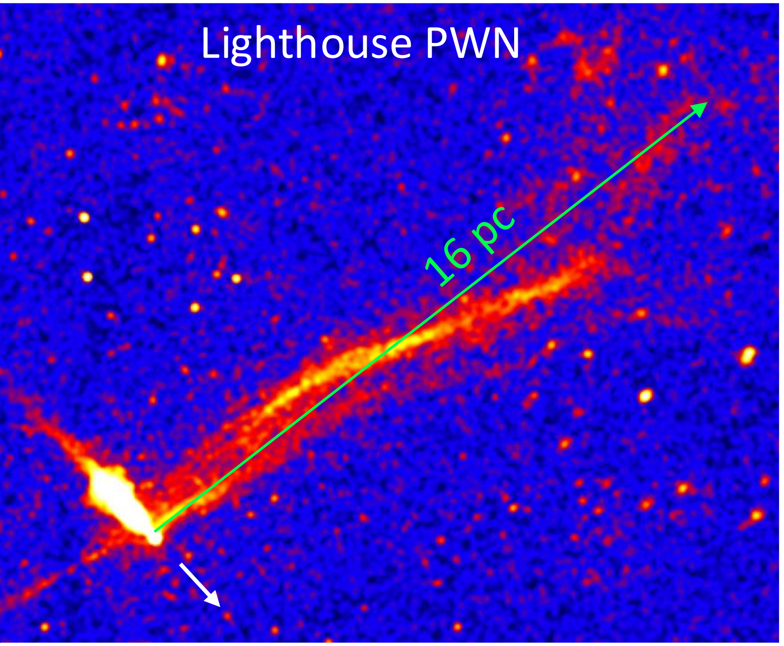

first two misaligned outflows identified

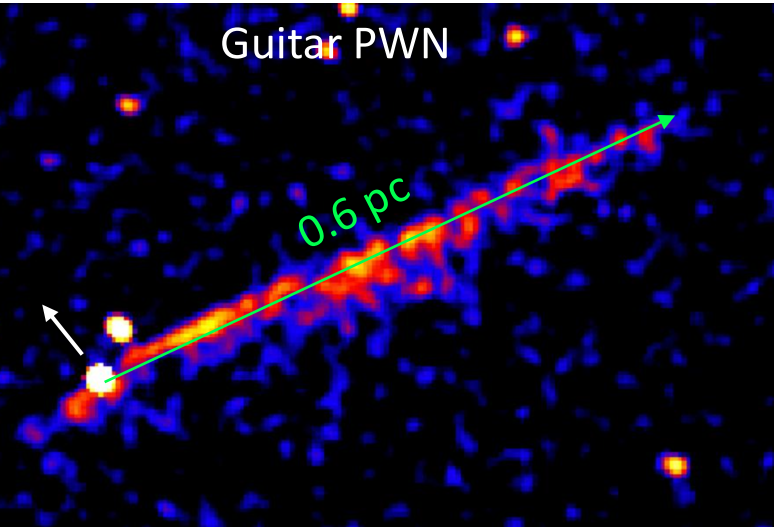

- associated with supersonic pulsars
- *strongly* misaligned from direction of pulsar motion
  - they are not pulsar tails
- appear unaffected by ram pressure, do not appear to bend!
- remain highly collimated over parsec-scale distances
- typically tens of times fainter than pulsar tails

  → difficult to detect → only a handful are currently known (~10)
- initially proposed that they might be powerful jets, with the counter-jet Doppler de-boosted
  - problem: jets should be (and are often seen to be) bent by ram pressure

c.f. “regular” supersonic PWNe (note the bent jets)

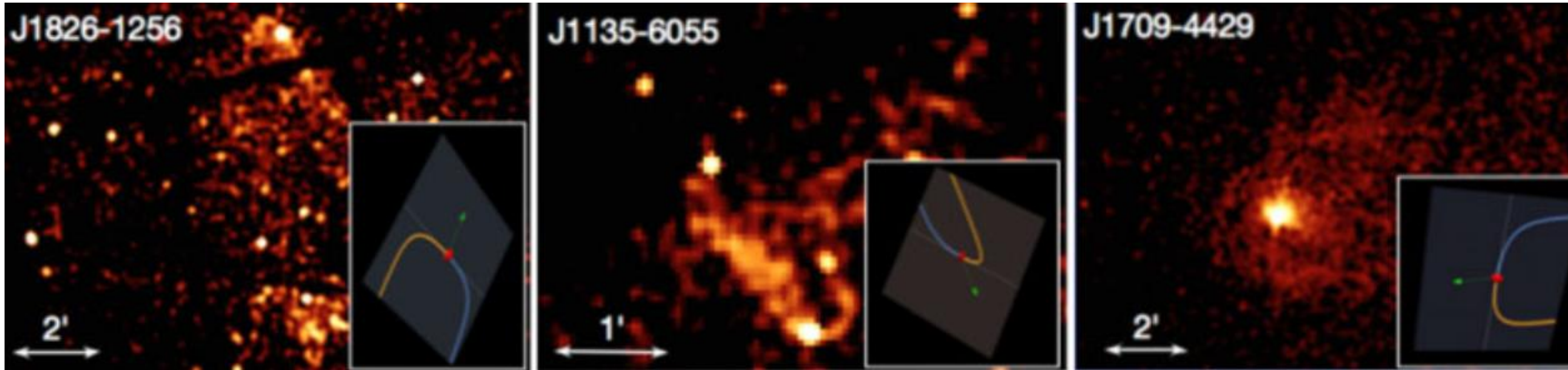

Misaligned Outflows

- but they are not pulsar jets (polar outflows)
  - jets are contained within the bow shocks

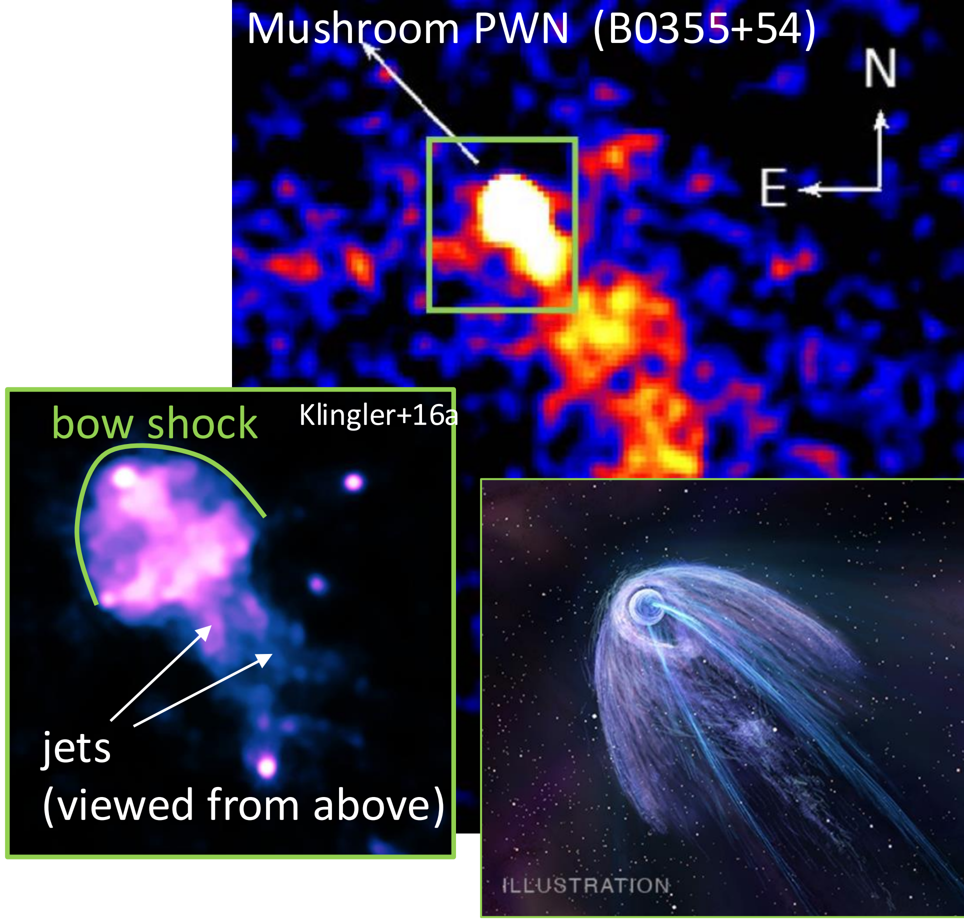

Klingler+16a

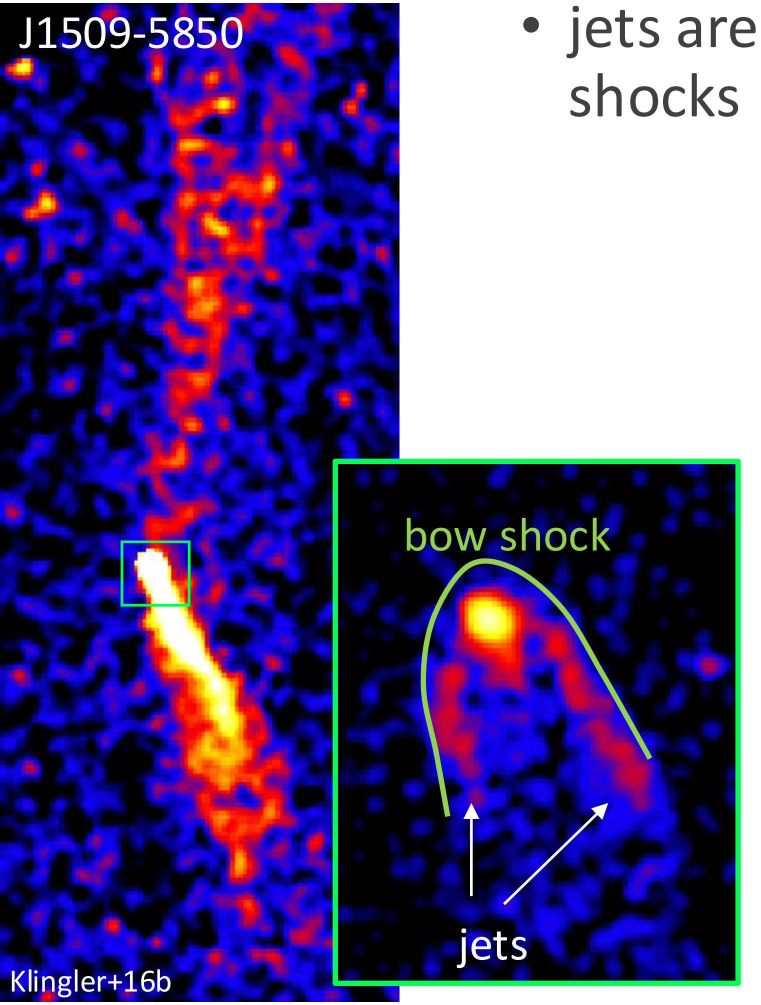

Klingler+16b

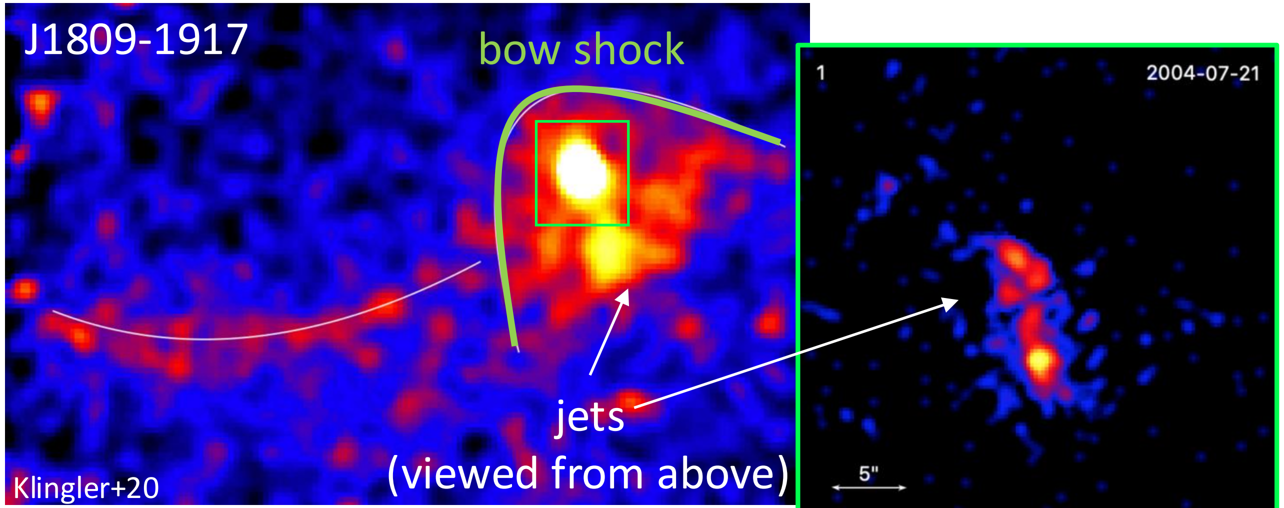

Klingler+20

Misaligned Outflows: Theory

- supersonic PWN interacts with external (ISM) magnetic field
    - B_{ISM} can “drape” around bow shock
    - same phenomenon seen around planets and Galaxy clusters, on scales millions of times smaller/larger
- simulations: ISM B-field can reconnect with PWN B-field
    - facilitates escape of particles
        - magnetic “bottle” screens out low-E particles
    - reconnection favors one side of PWN, since B-field is oriented in one direction

      → explains outflow one-sidedness

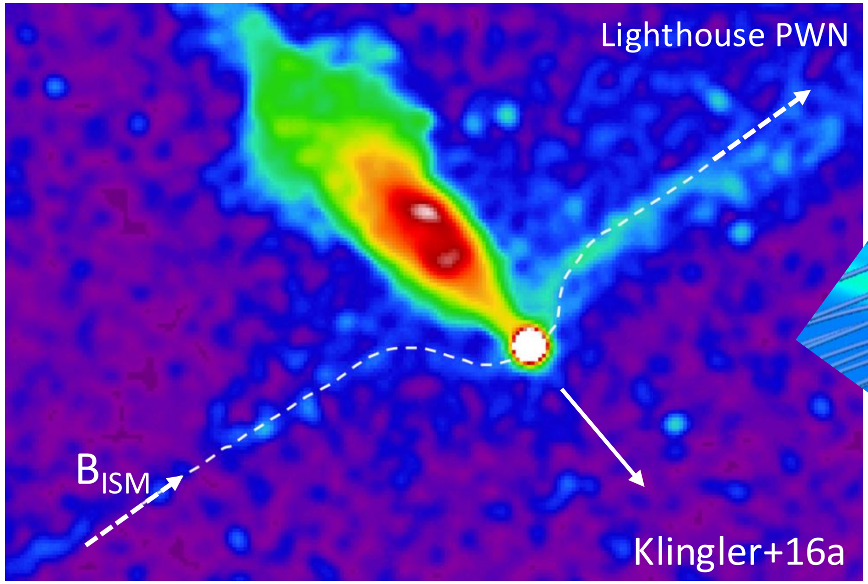

Klingler+16a

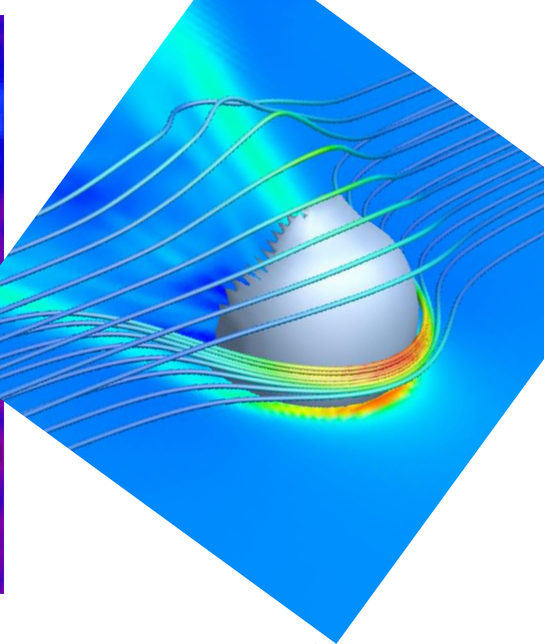

Dursi & Pfrommer 2010

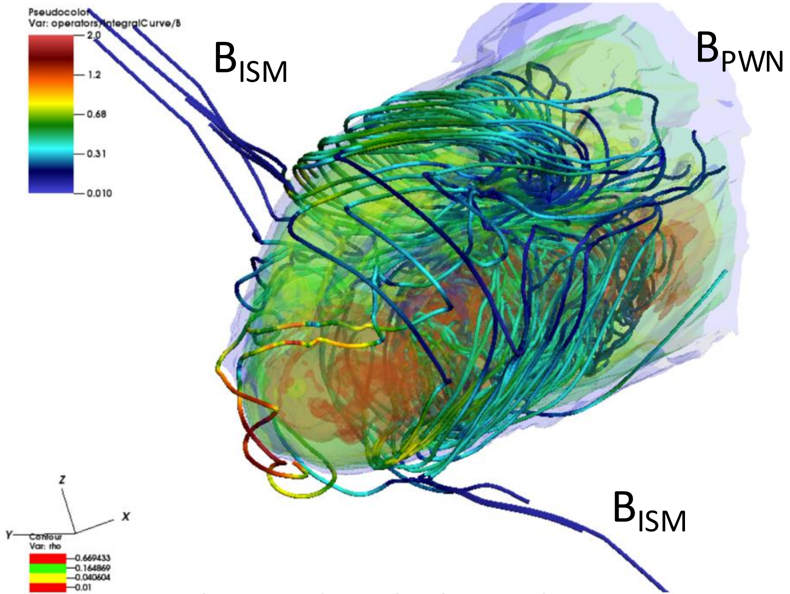

Barkov, Lyutikov, Klingler, Bordas 2019

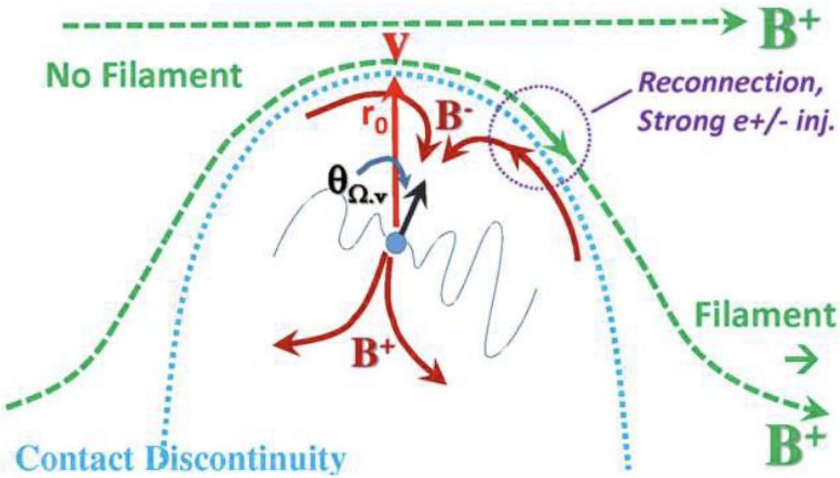

de Vries & Romani 2022

Case Study: The Lighthouse Nebula (PSR J1101-6101)

- d ~ 7 kpc
- age ~ 10-20 kyr
- $v_\perp$ ~ 1000 km/s

(possibly the fastest pulsar known)

- brightest and most luminous of the misaligned outflows

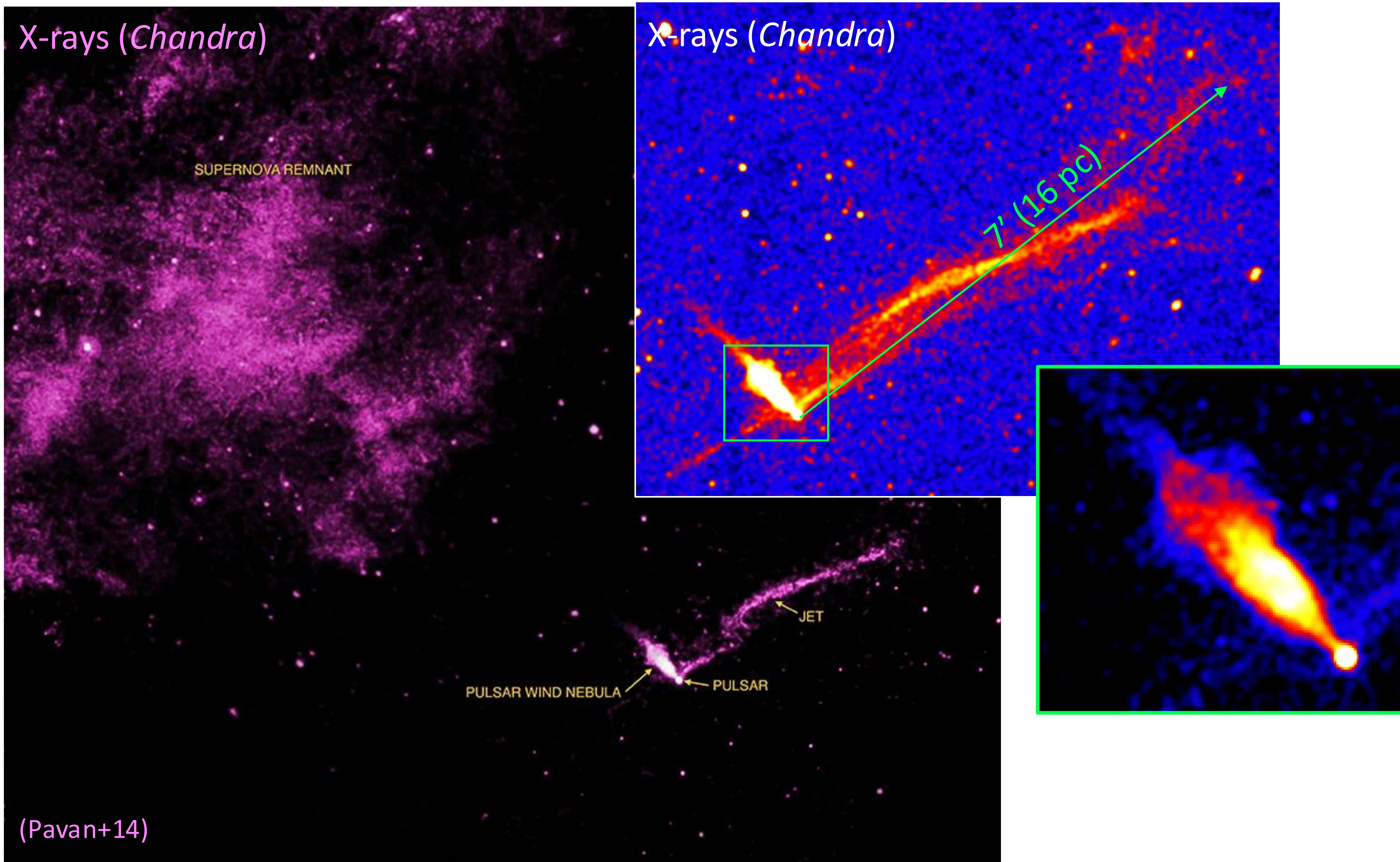

(Pavan+14)

Misaligned Outflows: Implications & Future Prospects

- misaligned outflows have been proposed as the high-energy analogs to the 100+ nonthermal radio filaments seen near the Galactic center (Barkov & Lyutikov 2019)
- pulsar particle leakage → multi-messenger astronomy: positron excess detected at Earth has been attributed to the nearby (d=250 pc) supersonic Geminga pulsar (Yüksel+09)

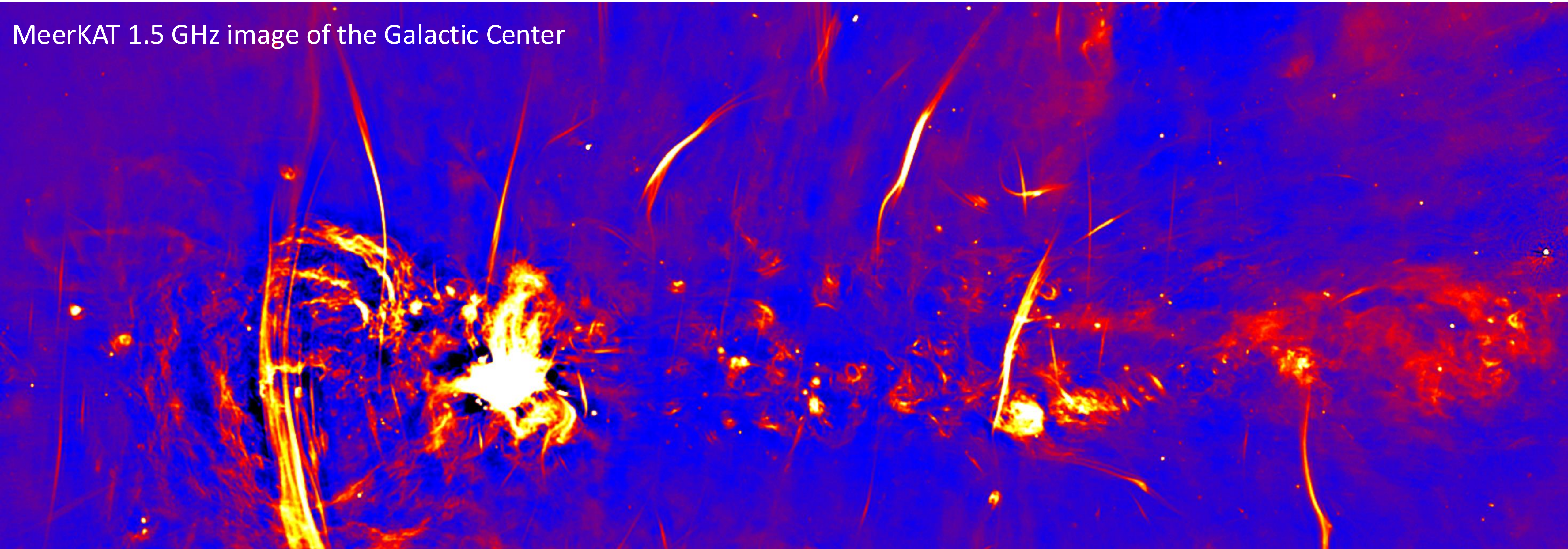
MeerKAT 1.5 GHz image of the Galactic Center

Summary

- misaligned outflows are a recently-discovered intriguing phenomenon observed in some fast-moving PWNe
- they represent the complex MHD interactions between supersonic pulsars and the ISM magnetic fields
  - also allow us to probe the properties of the ISM (density, magnetic field direction, and strength) which are otherwise difficult to do
- inform us about how pulsars seed the Galaxy with high-energy particles
- next-generation high-resolution X-ray observatories (like AXIS) will help us discover more of these faint structures and advance our understanding of the rich physics involved in these structures, and discover more instances

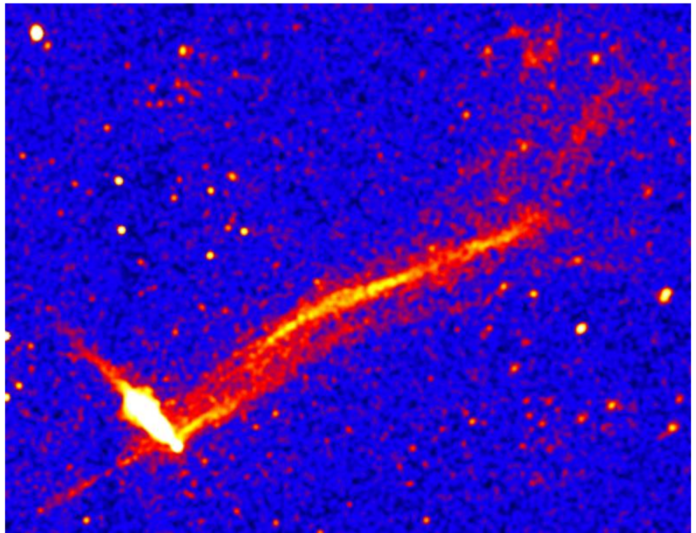

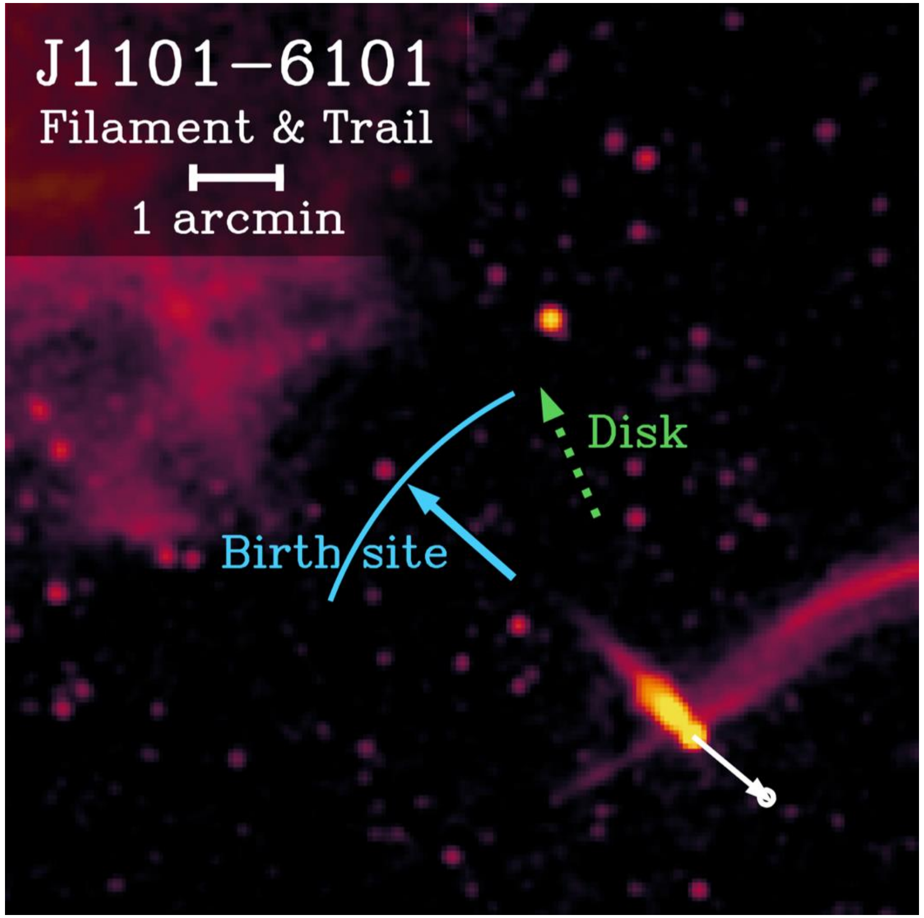
J1101−6101
Filament & Trail
1 arcmin
Disk
Birth site

Open questions:

- What does asymmetry tell us and why some supersonic PWNe are missing PFs?
- In Guitar PF escaping particle energies exceed full potential drop across the polar cap. Magnetic field amplification by a large factor despite the relatively low number of escaping particles?
- X-ray tail is missing in Guitar nebula, where are the particles with energies just below gating energy? Are their energies too low to emit X-rays even within the compressed pulsar tail?
- Could the PF particles come from ISM electron (not pulsar wind e^+e^-) begin accelerated in colliding flows (Bykov et al. 2017)?

Older PWN escaping from its host shell SNR

$\dot{E} = 3.4 \times 10^{36}$ erg s^{-1}
$\tau_c = 17$ kyrs
$B_s = 3.1 \times 10^{12}$ G

A torus-dominated PWN which appears to be surrounded by large scale faint X-ray emission which is offset from an even larger TeV emission region located behind the moving pulsar which still may be within its host SNR.

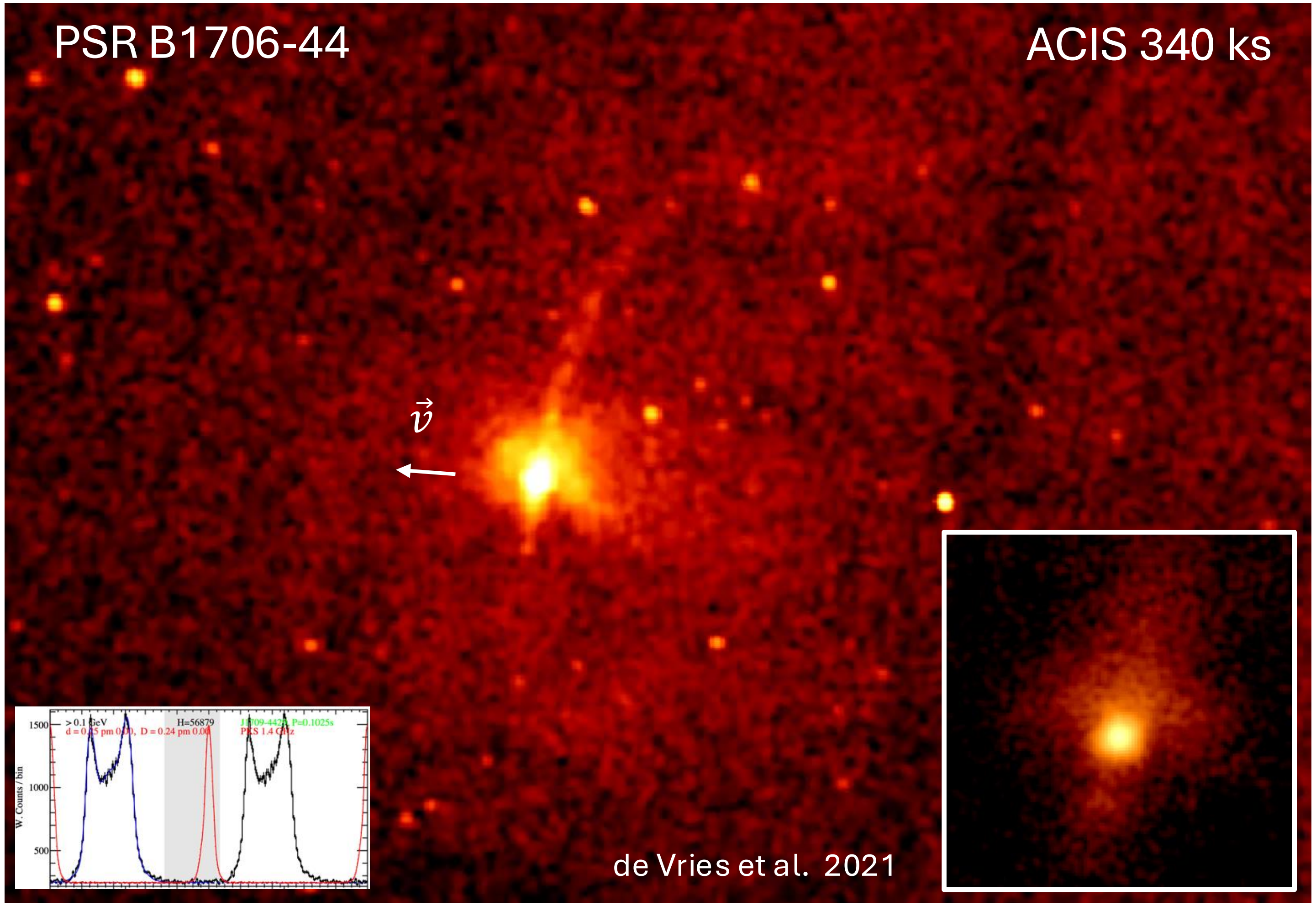

de Vries et al. 2021

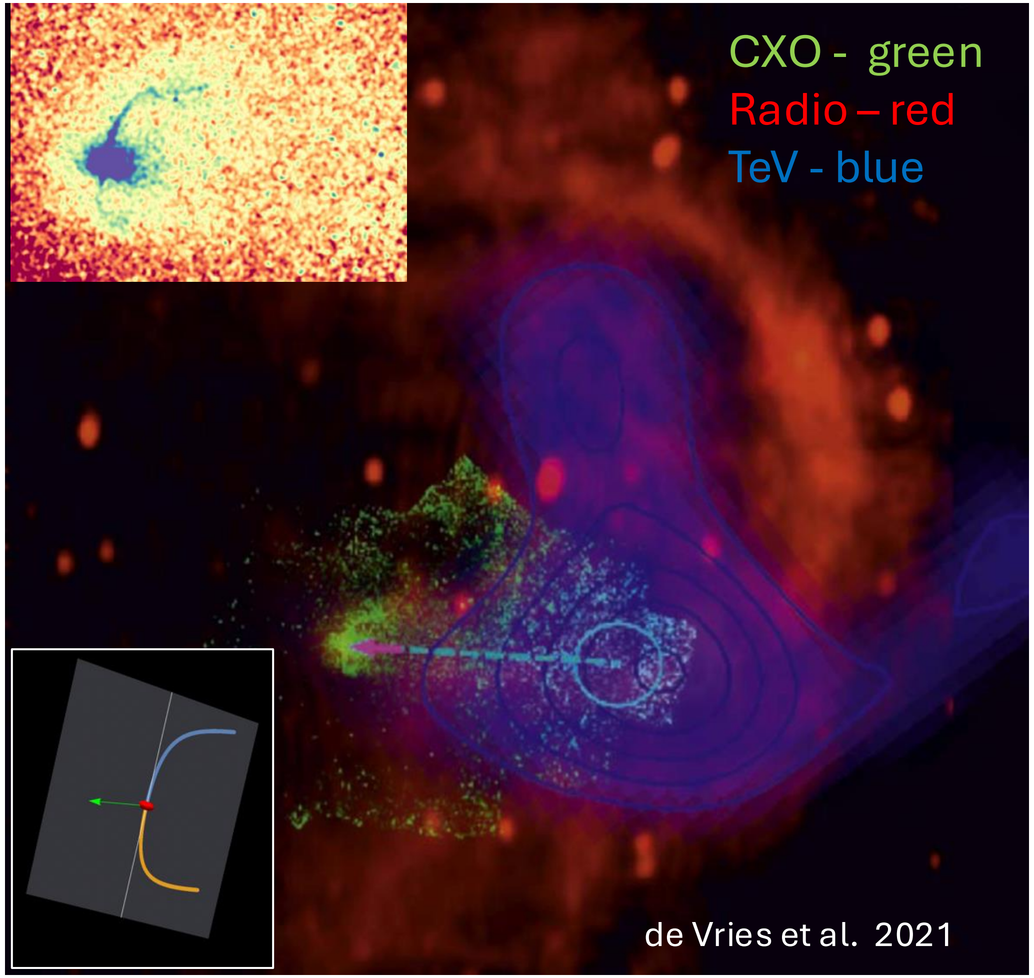

de Vries et al. 2021

MOA(s) of PSR J2055+2539

$\dot{E} = 5 \times 10^{33}$ erg s^{-1}
$\tau_c = 1{,}200$ kyrs
$B_s = 1.2 \times 10^{12}$ G

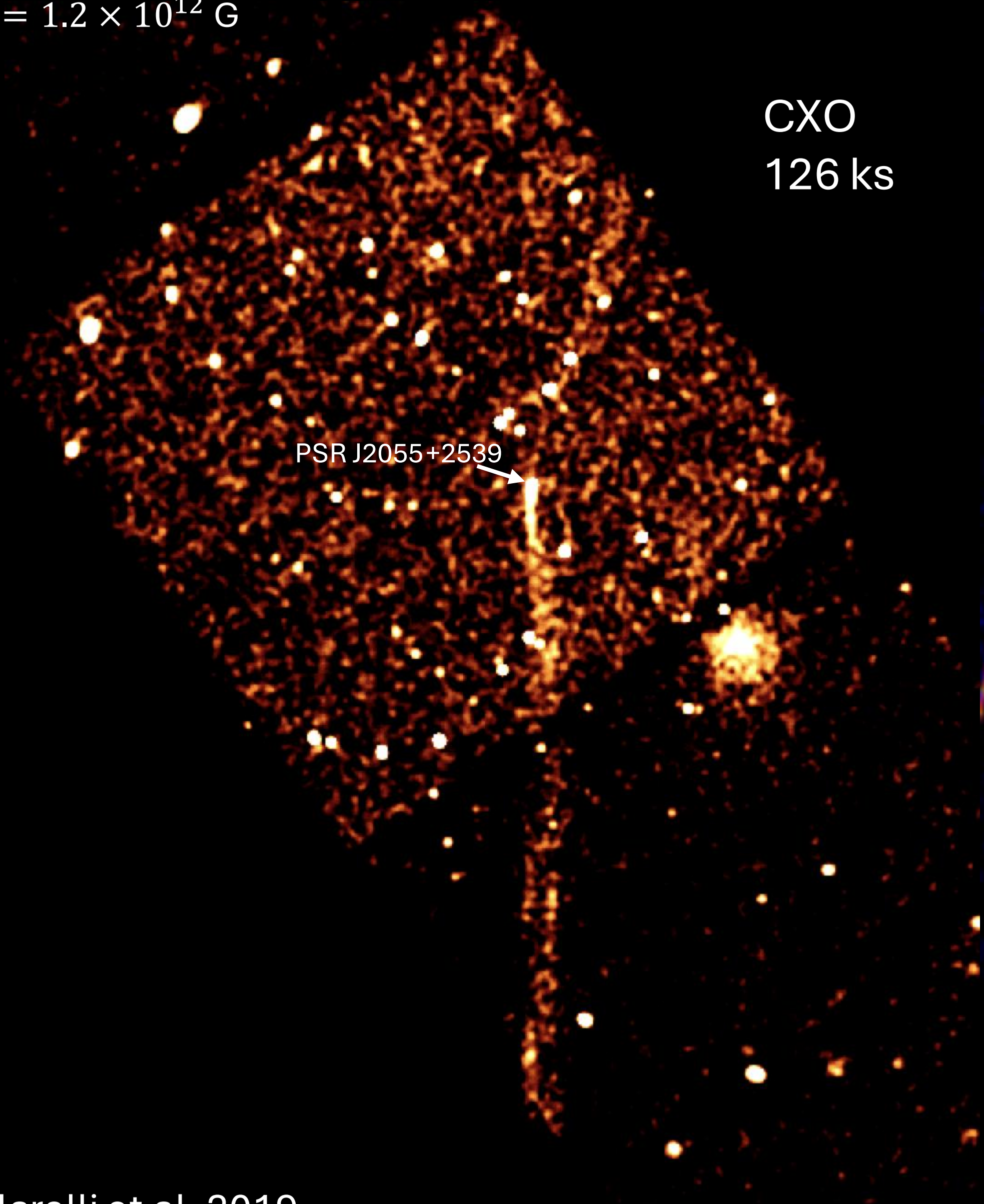

CXO
126 ks

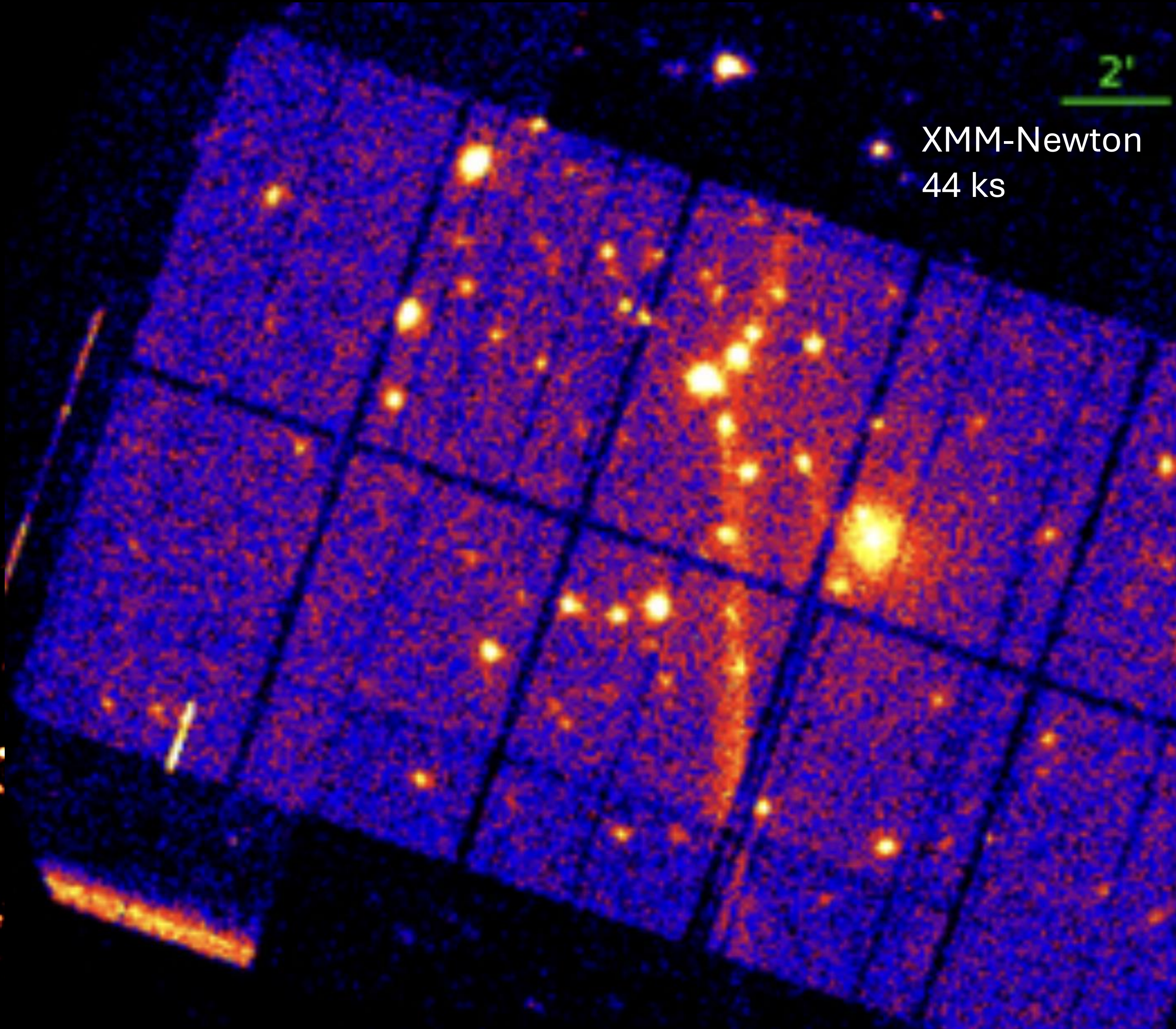

XMM-Newton
44 ks

Marelli et al. 2019

More examples of MOFs? But these show some evidence of bending with increasing distance from pulsar which one can expect form “fluid” jets…

MSH 15-56 PWN (see Temim, T., et al. 2017)

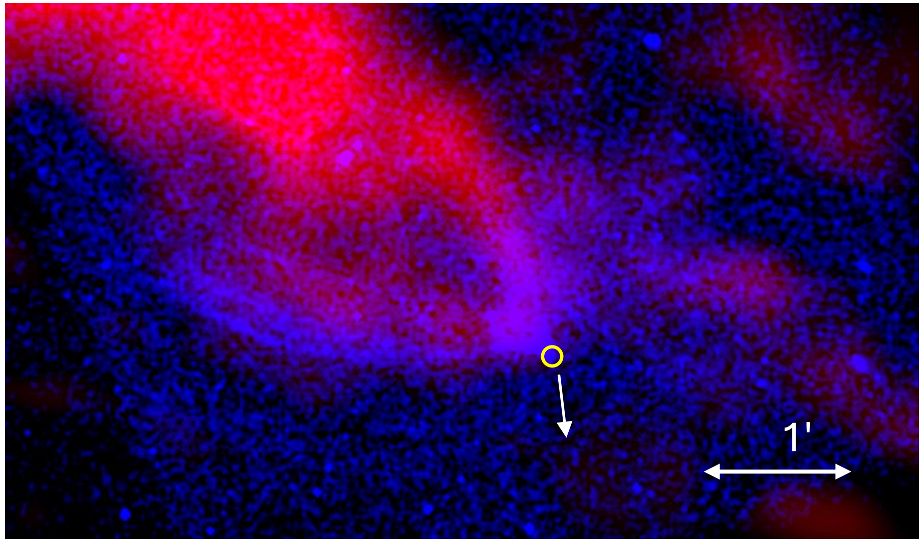

Tadpole (Klingler et al. 2020)

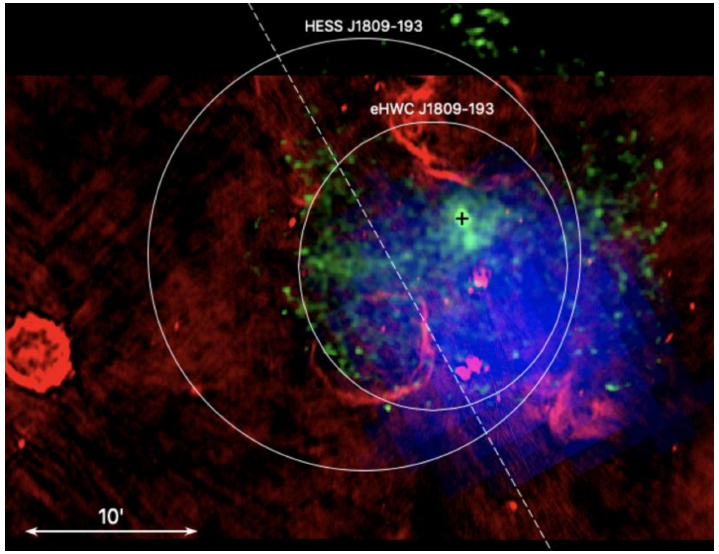

Dragonfly (Van Etten et al. 2008)

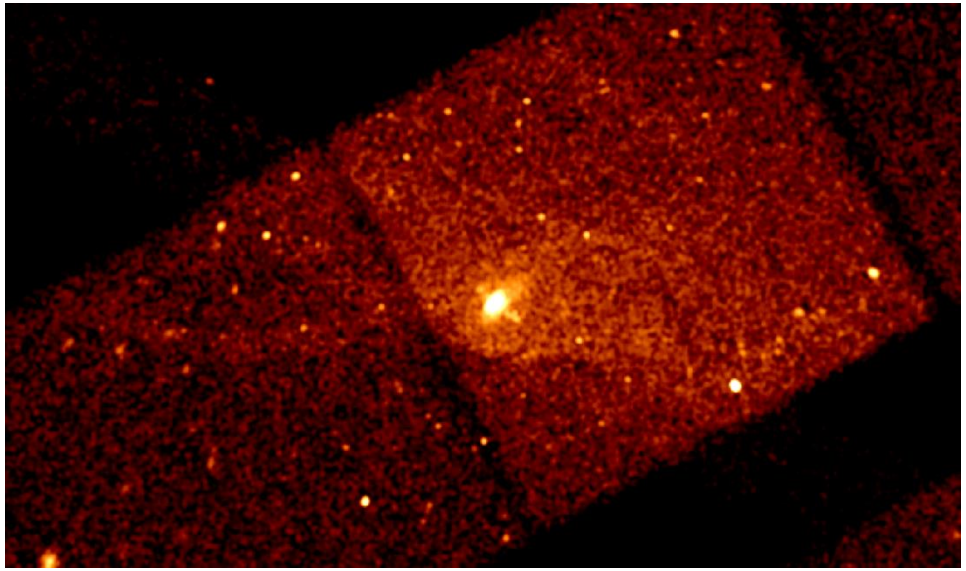

Geminga (Posselt et al. 2016)

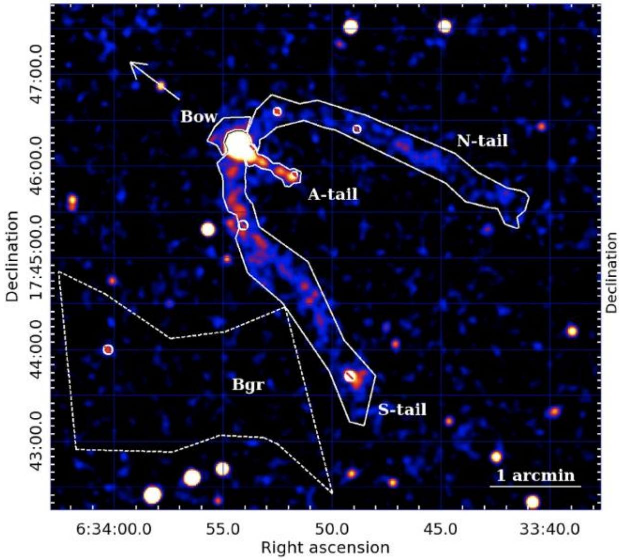

Evidence of magnetic field amplification in MOFs

Bandiera 2008; Olmi & Bucciantini 2019

- For some pulsars with MOFs γ_{esc} is too large compared to polar cap voltage, if ISM magnetic field is assumed.
- For some MOFs the width is too narrow, if B-field is a typical ISM field (both from gyro-radius and cooling time arguments).
- Theoretical work and numerical simulations also suggest B-field amplification.

Alternative:

Acceleration of ISM electrons either between the FS and CD near the PWN apex in which case the pulsar's kinetic energy can be tapped into. A possible evidence of this is the X-ray emission seen up to ~ 3" ahead of the Lighthouse pulsar while the expected standoff distance is

$$r_s \simeq 0.08''(\mu/50\,\mathrm{mas/yr})n_{\mathrm{H}}^{-1/2}(d/7\ \mathrm{kpc})^{-2}\sin i$$

Filaments near Galactic Center.

Red – radio; green – X-rays

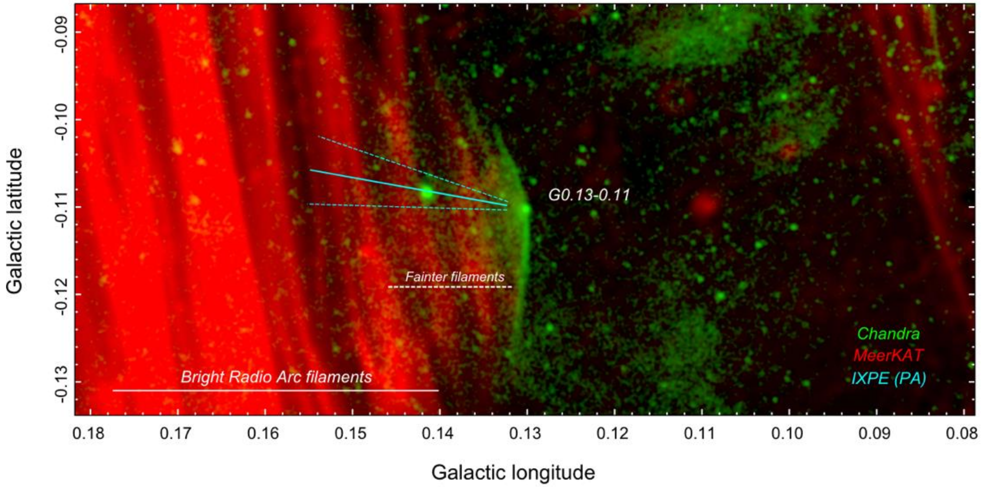

Churazov et al. 2024

Can old PSRs or MSPs have MOFs?

PSR J1744−2946 is a binary MSP

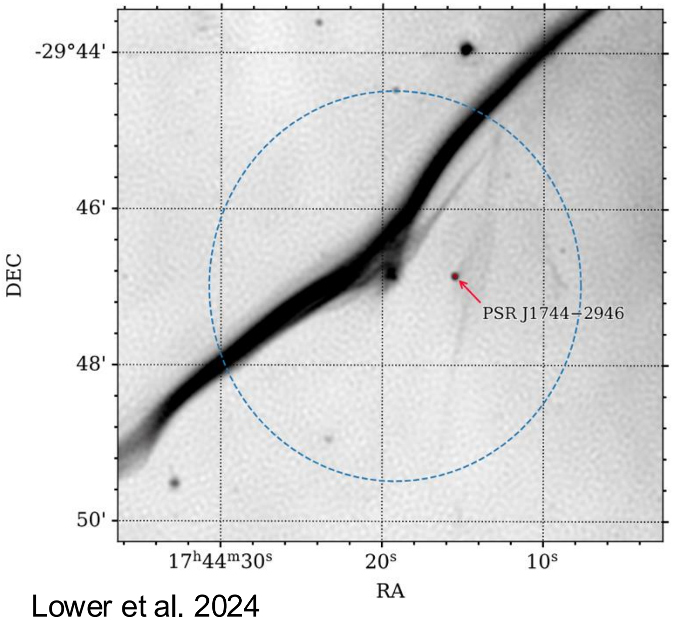

Lower et al. 2024

Figure 1. 1.28 GHz radio image of the region around the major kink

For pulsars with lower Edot misaligned outflows could be seen at lower frequencies due to the larger bow shock apex stand-off distances.

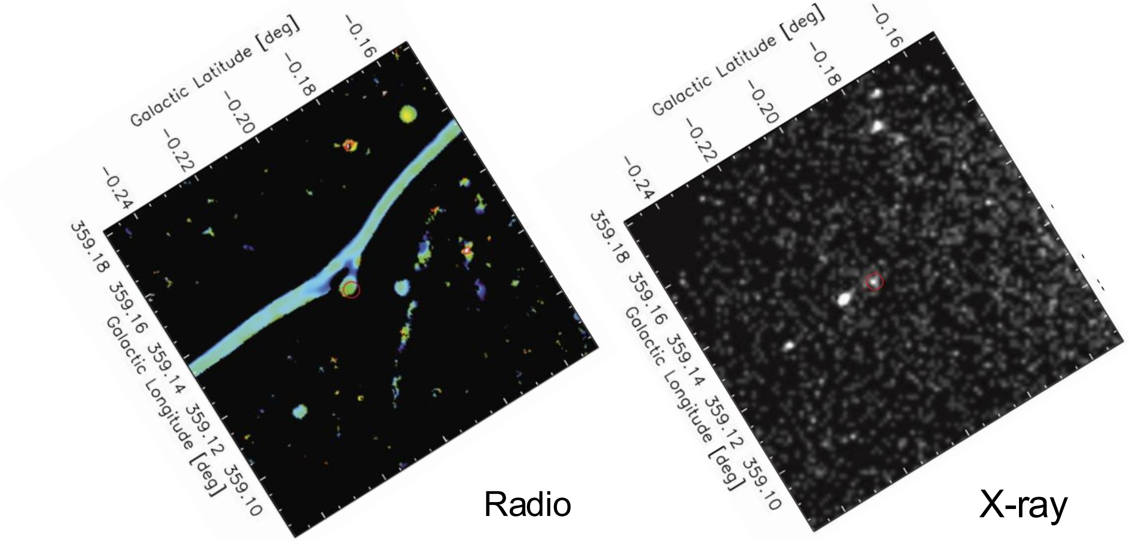

Radio

X-ray

Yusef-Zadeh et al. 2024

X-ray PWN + H-alpha bow shock

5 (6?) known, out of 9 PSR H-alpha bow shocks

3 examples

PSR B1957+20 (black widow)
Stappers et al 2003

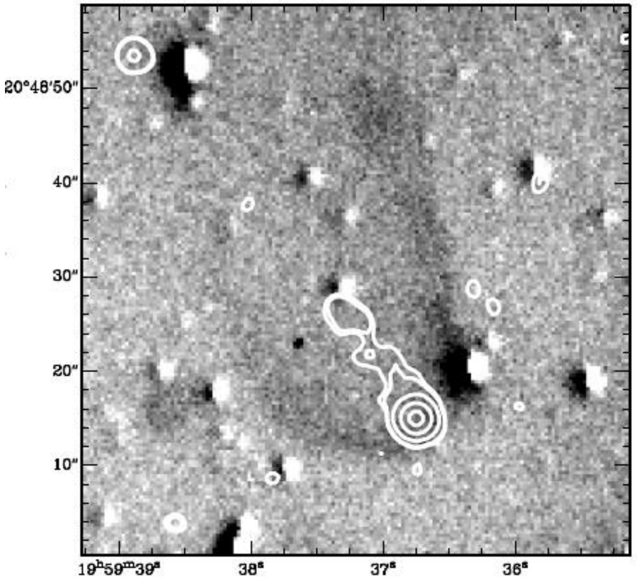

Head-tail X-ray PWN within H-alpha bow shock

PSR B2224+55 (Guitar)
Johnson & Wang 2010

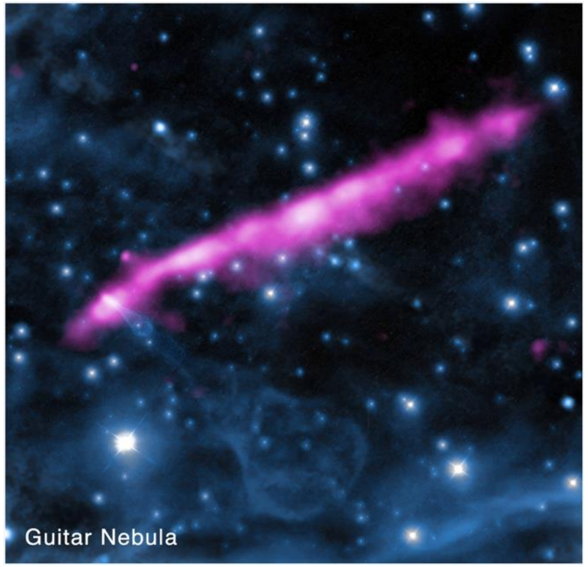

Misaligned outflow in X-rays, bow shock + several bubbles In H-alpha

PSR J2124-3358, solitary MSP
Chatterjee et al 2009

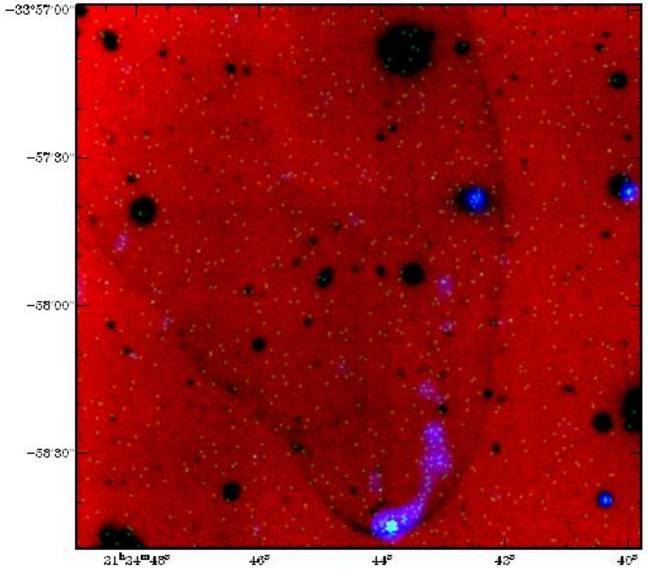

One-sided X-ray “jet” within asymmetric H-alpha bow shock

A nice hydrodynamic (fluid) jet example:

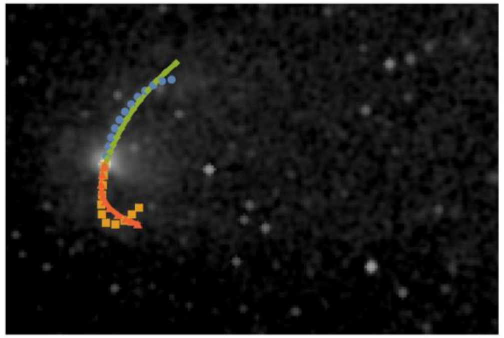

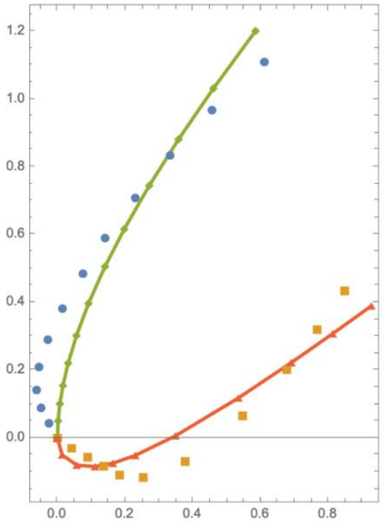

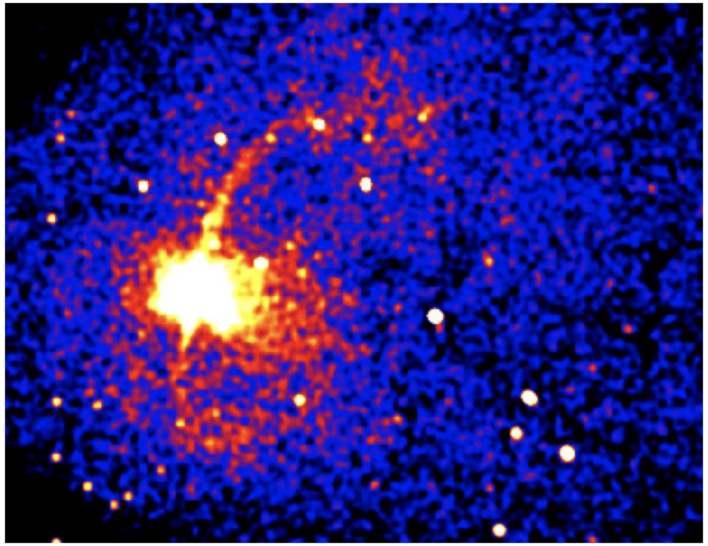

de Vries et al. (2020)
https://arxiv.org/abs/2012.00048

Cross-wind force balance

$$\frac{mv^2}{R} = \rho(w\sin\alpha)^2 dl D \qquad \vec{v(s)} = (v_x(s), v_y(s))$$

$$\frac{1}{R\sin^2\alpha} = \frac{\sqrt{v_x'^2 + v_y'^2}}{v_y^2} = \frac{\beta}{D}$$

where β is the ratio of momentum flux in the jet to the ISM momentum flux across the jet

$$\beta \ = \ \rho w^2 c D^2/(\xi \dot{E})$$

Solution:

$$x(s) = \sqrt{1+(s-g\cot\theta)^2} - \frac{1}{\sin\theta},$$
$$y(s) = g\sinh^{-1}(s-g\cot\theta) + \sinh^{-1}(\cot\theta).$$

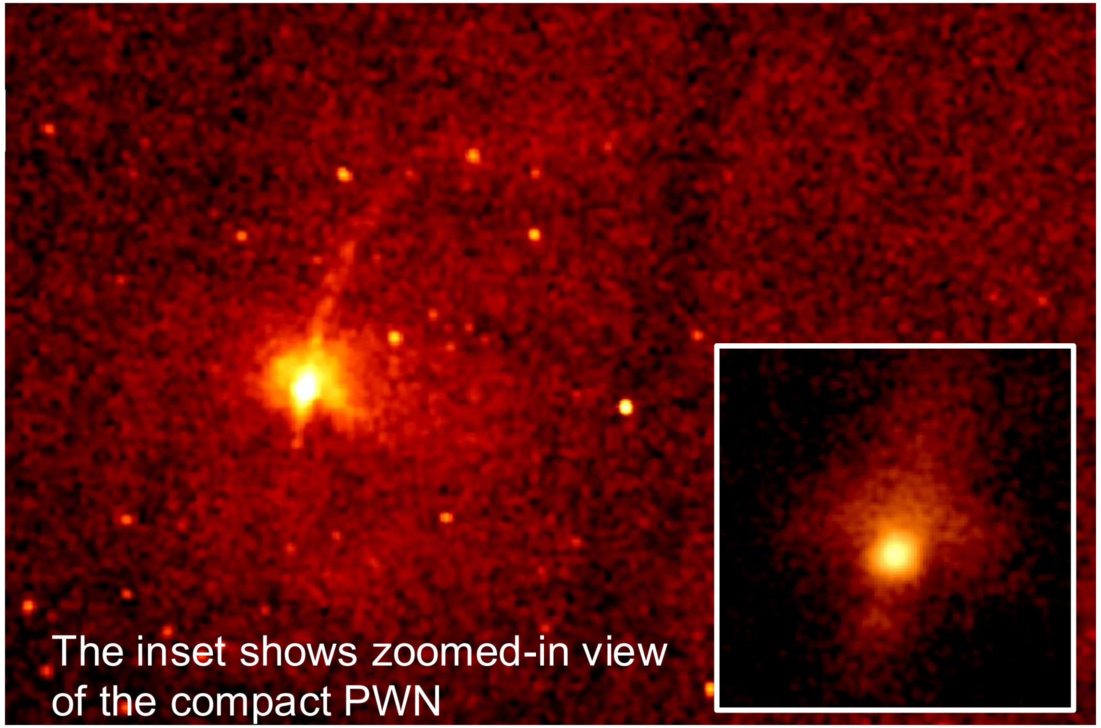

The inset shows zoomed-in view of the compact PWN